Journal of Bioresources and Bioproducts xxx (xxxx) xxx

Contents lists available at ScienceDirect

Journal of Bioresources and Bioproducts

journal homepage: www.elsevier.com/locate/jobab

# Synthesis and application of Granular activated carbon from biomass waste materials for water treatment: A review

Joseph Jjagwe[a], Peter Wilberforce Olupot[a,*], Emmanuel Menya[b], Herbert Mpagi Kalibbala[c]

[a] Department of Mechanical Engineering, College of Engineering, Design, Art and Technology, Makerere University, P.O. Box 7062, Kampala-Uganda
[b] Department of Biosystems Engineering, Gulu University, P.O. Box 166, Gulu, Uganda
[c] Department of Civil and Environmental Engineering, College of Engineering, Design, Art and Technology, Makerere University, P.O. Box 7062, Kampala-Uganda

ARTICLE INFO

*Keywords:*
Activated carbon
Biomass waste
Binder
Water treatment
Adsorption mechanism
Regeneration

ABSTRACT

There is an increased global demand for activated carbon (AC) in application of water treatment and purification. Water pollutants that have exhibited a greater removal efficiency by AC included but not limited to heavy metals, pharmaceuticals, pesticides, natural organic matter, disinfection by-products, and microplastics. Granular activated carbon (GAC) is mostly used in aqueous solutions and adsorption columns for water treatment. Commercial AC is not only costly, but also obtained from non-renewable sources. This has prompted the search for alternative renewable materials for AC production. Biomass wastes present a great potential of such materials because of their availability and carbonaceous nature. This in turn can reduce on the adverse environmental effects caused by poor disposal of these wastes. The challenges associated with biomass waste based GAC are their low strength and attrition resistance which make them easily disintegrate under aqueous phase. This paper provides a comprehensive review on recent advances in production of biomass waste based GAC for water treatment and highlights future research directions. Production parameters such as granulation conditions, use of binders, carbonization, activation methods, and their effect on textural properties are discussed. Factors influencing the adsorption capacities of the derived GACs, adsorption models, adsorption mechanisms, and their regeneration potentials are reviewed. The literature reveals that biomass waste materials can produce GAC for use in water treatment with possibilities of being regenerated. Nonetheless, there is a need to explore 1) the effect of preparation pathways on the adsorptive properties of biomass derived GAC, 2) sustainable production of biomass derived GAC based on life cycle assessment and techno-economic analysis, and 3) adsorption mechanisms of GAC for removal of contaminants of emerging concerns such as microplastics and unregulated disinfection by-products.

## 1. Introduction

Activated carbon (AC) is a microporous form of carbon with a well-developed pore structure, pore volume, high internal surface area, and consequently a high adsorption capacity (Galvão et al., 2020; Lu et al., 2020; Hao et al., 2021). The AC also exhibits functional groups on its surface, which influences the solution pH, and consequently the adsorption process (Mallek et al., 2018; Alharbi et al., 2020). The AC finds wide applications in water treatment and purification, where adsorption mechanisms such as

* Corresponding author.
*E-mail address:* polupot@cedat.mak.ac.ug (P.W. Olupot).

https://doi.org/10.1016/j.jobab.2021.03.003
Received 29 December 2020; Received in revised form 15 February 2021; Accepted 22 February 2021
Available online xxx


Please cite this article as: J. Jjagwe, P.W. Olupot, E. Menya et al., Synthesis and application of Granular activated carbon from biomass waste materials for water treatment: A review, Journal of Bioresources and Bioproducts, https://doi.org/10.1016/j.jobab.2021.03.003

physisorption and/or chemisorption allow contaminants to shift from the liquid to the solid surface (Lima et al., 2016; Dai et al., 2020). The wide application of the AC in water treatment and purification is due to its relatively high adsorption performance and usability, prompting its application as a potential alternative to the conventional and advanced water treatment technologies (Liu et al., 2020a). The advanced technologies are not only unevenly distributed worldwide (Palansooriya et al., 2020), but also associated with high operational and maintenance costs (Talat et al., 2018).

Commercially, ACs have been widely obtained from non-renewable sources such as coal, lignite, and peat. These exhibit a low mineral content, high carbon content, as well as a high porosity, which suit them as AC precursors (Teng and Lin, 1998). However, due to their associated environmental and economic concerns, there is an increased research interest to find low-cost biomass waste materials, as well as low-cost processes for production of AC (Plaza-Recobert et al., 2017; Gonçalves et al., 2019). More specifically, in developing countries, agricultural and industrial wastes present a huge potential as precursors for AC production (Yang and Qiu, 2011; Thakur et al., 2020). This is due to their wide availability, low-cost (Tran et al., 2019; Santoso et al., 2020) and their carbonaceous nature (Kaur et al., 2019; Karri et al., 2020). Deploying biomass wastes as AC precursors provides a sustainable waste disposal option, as opposed to the common practice of open burning and/or waste deposition (Mohamed Nor et al., 2013; Abo El Naga et al., 2019). Open burning of wastes emits particulate matter and obnoxious gases, polluting the environment, while open waste deposition causes blockage of drainage channels during rainy seasons. The deposited wastes also serve as breeding grounds for pathogens (Chou et al., 2009). With the judicious selection of biomass waste, preparation methods, as well as careful control of preparation and adsorption conditions, biomass waste-derived ACs exhibit superior adsorption performance, as compared to their commercial counterparts (Huggins et al., 2016; Tran et al., 2019).

The AC is marketed in two forms namely, powdered activated carbons (PACs) and granular activated carbons (GACs). The PACs usually exhibit high specific surface area and micro-porosity which increases their adsorption capacity (Alslaibi et al., 2013; Deng et al., 2015). Nevertheless, the small particles of PAC present slower settling and removal tendencies than GAC (Dias et al., 2007). In spite of its higher adsorption capacity, the PAC can not be regenerated due to difficulties in separating it from the aqueous solution (Deng et al., 2015), as well as due to the potentially high rates of dust pollution (Cai et al., 2020). Because of these difficulties, the PACs are typically employed in batch modes especially in water treatment facilities (Jaria et al., 2019). In designs where continuous columns are more feasible in water treatment, and regeneration of the carbons is of important consideration for environmental and economic reasons, the GACs are the best suited form of ACs. This is due to GAC's adaptability to continuous contacting with no need to separate the carbon from the bulk fluid (Yuan and Sun, 2010). Compared with the PAC, GAC typically exhibits lower adsorption capacities for pollutant removal from aqueous solutions (Ali et al., 2010; Cai et al., 2020). This adsorption tendency by the GACs is due to the fouling effect, as well as to the reduced mass transfer of the target pollutants (Meinel et al., 2014).

The GAC is currently used as a water treatment material to effectively remove a number of pollutants including organic micro-pollutants (Brunner et al., 2020), pharmaceuticals (Lima et al., 2016), arsenic (Kalaruban et al., 2019), carcinogenic compounds (Myers et al., 2018), microplastics (Wang et al., 2020d), heavy metals (Eeshwarasinghe et al., 2019), colour and odour (Ziemba et al., 2020). The choice for GAC depends on the target pollutant, concentration of the pollutant, flow rate, and adsorption capacity (Kårelid et al., 2017). The aforementioned factors also influence the life span of the carbon (Huggins et al., 2016). Given the importance and relevance of GAC from biomass materials elucidated in the foregoing sections, this paper reviews the various methods for GAC production from biomass waste materials, their characterization, and appraisal protocols for their application in pollutant removal from water. The regeneration potential of biomass waste-derived GACs and future research directions that need to be addressed are cited.

## 2. Methodology

Databases of Google Scholar and Web of Science were searched through selected keywords to obtain original articles, review articles, book chapters, and scientific reports for review purposes to contribute to this work. The key words were searched individually and/or in combinations of up to three terms. The most prevalent keywords included activated carbon, powdered activated carbon, granular activated carbon, pellets, binders, granules, water treatment, adsorption kinetics, isotherms, and mechanisms, physical activation, chemical activation, hydrothermal carbonization, microwave carbonization, contaminants of emerging concern, and regeneration. Boolean operators AND, "", and () were mainly employed to obtain the most relevant articles of the search subject. Studies were mainly selected if the AC under investigation was from biomass waste(s) with particle size in the range of 0.2–5.0 mm. Another selection criterion was based on the general aspects that cut across all ACs such as material suitability for activated carbon, pretreatment, carbonization and activation, as well adsorption mechanisms. Due to the vast amount of literature available concerning the production of AC from biomass wastes, mostly articles published from 2010 to date were considered. Articles published before 2010 were only included if; 1) they were deemed necessary to support/contradict other studies, and 2) the contents were exclusive and worth highlighting. Titles of over 600 papers were scanned and about 500 papers were screened before relevant scientific publications amounting to 302 papers were eventually selected for this review.

## 3. Material selection for AC production

The nature of raw material has a significant influence over the properties of the resultant AC, making material selection one of the most important factors that needs to be carefully considered in the production of AC. Material selection is based on factors such as availability, accessibility, purity as well as the extent of activation (Ahmed and Theydan, 2012). The lignocellulosic, proximate, and ultimate compositions of biomass waste commonly employed as AC precursors are shown in Table 1. From Table 1, it can be

**Table 1**
Ultimate, proximate and lignocellulosic compositions of biomass waste commonly employed as activated carbon (AC) precursors.

| Biomass waste type | Ultimate composition (% ad)[a] | | | | | Proximate composition (% ad)[a] | | | | Lignocellulosic composition (% ad)[a] | | | Reference |
|---|---|---|---|---|---|---|---|---|---|---|---|---|---|
| | C | H | N | S | O[b] | MC | VM | FC | Ash | Lignin | Hemicellulose | Cellulose | |
| Rice straw | 39.2–42.9 | 5.3–5.8 | 0.5 –1.1 | 0.1 | 34.3–50.7 | 7.1–9.3 | 63.9–72.1 | 5.5–20.9 | 14.7–15.4 | 10.2–12.4 | 7.8–31.1 | 33.9–51.5 | (Li et al., 2020a; Tian et al., 2020; Wei et al., 2020) |
| Rice husks | 35.6–46.8 | 3.6–5.0 | 0.8–2.4 | 0.1 | 47.1–59.8 | 6.3–7.2 | 58.7–73.1 | 4.4–20.6 | 14.2–17.3 | 18.3–26.0 | 19.0–25.1 | 32.0–45.6 | (Kumar et al., 2019; Gajera et al., 2020; Naqvi et al., 2020) |
| Wheat straw | 45.3–48.2 | 5.6–5.7 | 0.4–0.6 | 0.4 | 44.6–48.8 | 5.2–7.7 | 66.8–78.3 | 7.0–20.6 | 3.9–9.2 | 18.0–25.7 | 21.2–36.0 | 35.0–37.5 | (Ma et al., 2018; Kumar et al., 2019; Naqvi et al., 2020) |
| Sugarcane bagasse | 39.8–46.2 | 5.8–6.1 | 0.5–0.6 | 0.2 | 46.7–53.6 | 7.4–8.7 | 69.8–81.0 | 4.3–15.5 | 4.1–8.1 | 12.0–24.0 | 24.8–32 | 24.8–44.0 | (Kumar et al., 2019; Naqvi et al., 2020; Siddiqi et al., 2020a) |
| Peanut shell | 48.3–51.1 | 4.5–6.5 | 1.1–1.8 | 0.1–0.5 | 38.5–42.1 | 4.7–6.7 | 61.7–73.8 | 18.6–27.2 | 2.9–5.9 | 26.4–30.9 | 14.5–18.7 | 30.9–40.5 | (Gurevich Messina et al., 2017; Bhatnagar et al., 2020; Jiang et al., 2020) |
| Coconut shell | 47.4 | 5.1–6.6 | 0.4–0.5 | 0.2 | 37.2–45.3 | 4.3–10.3 | 72.9–73.5 | 11.9–18.8 | 4.0–4.3 | 30.2–35.1 | 34.1–38.0 | 18.7–27.2 | (Siddiqi et al., 2020b; Wei et al., 2020) |
| Corn cob | 44.1–46.9 | 5.1–6.5 | 0.7–0.8 | 0.1 | 43.7–48.6 | 5.1–23.6 | 72.6–82.1 | 5.3–16.1 | 2.7–11.7 | 4.2–44.6 | 25.7–39.2 | 7.9–40.3 | (Martínez et al., 2020; Naqvi et al., 2020; Siddiqi et al., 2020a) |
| Corn stalk | 43.6–46.4 | 5.8–6.7 | 0.9–1.4 | 0.2 | 16.2–46.0 | 4.8 | 72.2–79.2 | 11.1–21.6 | 4.9–6.2 | 30.1–30.1 | 34.8–38.5 | 13.9–27.3 | (Patowary and Baruah, 2018; Kang et al., 2019; Wan et al., 2019) |
| Palm kernel shell | 45.2–50.7 | 4.9–6.0 | 0.3–0.4 | 0.1 | 40.8–43.6 | 4.9–7.4 | 69.8–79.2 | 13.7–22.7 | 1.1–2.2 | 47.7 | 22.3 | 27.6 | (Mohd Faizal et al., 2018; Acevedo-Páez et al., 2020; Chang et al., 2020) |
| Cotton stalk | 39.6–49.6 | 3.2–6.0 | 0.4–0.9 | 0.4–0.5 | 46.0–47.6 | 10.6 | 75.1 | 11.3– 19.5 | 2.9–6.5 | 30 | 25 | 43 | (Gupta et al., 2020; Song et al., 2020) |
| Banana peel | 40.0–40.7 | 5.7–7.1 | 0.7–1.4 | 0.1 | 52.1–52.6 | 9.5–9.7 | 62.6–85.6 | 0.1–14.5 | 1.9–13.4 | 24.3 | 10.5 | 40.2 | (Pathak and Mandavgane, 2015; Saha et al., 2016; Ozbay et al., 2019) |
| Coffee husk | 45.3–46.4 | 6.2–6.3 | 0.6–2.7 | 0.1 | 43.7–44.5 | 9.1 | 77.1–82.7 | 16.2–19.4 | 2.4–3.6 | 25.4–27.1 | 17.8 | 36.0 | (Gebresemati et al., 2017; Setter et al., 2020) |
| Pine sawdust | 46.1–53.5 | 5.8–6.9 | 0.2–3.3 | 0.7 | 32.6–47.2 | 7.9–8.3 | 75.0–77.3 | 10.6–12.2 | 0.5–2.9 | 12.6–29.3 | 16.4 | 52.52 | (Yang et al., 2019; Ellison et al., 2020) |
| Jackfruit peel | 48.8 | 5.5 | 1.3 | 0.4 | 46.4 | – | 81.2 | 13.2 | 5.6 | 20.4 | 16.3 | 22.8 | (Alves et al., 2020) |

Notes: a, based on air dried basis; b, obtained as a difference; C, carbon; H, hydrogen; N, nitrogen; S, Sulphur; O, oxygen; MC, moisture content; VM, volatile mater; FC, fixed carbon.

seen that there are variations in the characteristics of the biomass wastes, even among those of the same type, suggesting that the preparation methods for AC may not be directly transferrable from one material to another.

### 3.1. Lignocellulosic composition

The lignocellulosic components of biomass include lignin, hemicellulose and cellulose, which on a dry basis range from 4%–50%, 8%–40%, and 8%–53%, respectively, depending on the biomass type (Table 1). In the production of AC, a high lignin concentration is desirable since lignin is richer in carbon content than either cellulose or hemicellulose. Lignin is the major component that contributes to the yield of AC (Gurevich Messina et al., 2017; Başakçılardan Kabakcı and Baran, 2019). Depending on the precursor, the weight contribution of lignin to AC ranges between 53.5%–78.8%, hemicellulose 13.6%–23.6% and cellulose 6.2%–30% (Cagnon et al., 2009). The yield of char and hence AC increases with increased lignin content. This is because lignin is thermally stable at higher temperatures due to the existence of functional groups such as $–OCH_3$ that are prone to charring (Kwon et al., 2020). On the other hand, cellulose and hemicellulose are the volatile fractions removed during pyrolysis, and are associated with low carbon yields since a significant fraction of carbon is lost during pyrolysis.

### 3.2. Proximate and ultimate compositions

Biomass suitable for carbonization should have a moisture content not exceeding 30wt%, as this reduces the need for heat energy and time that would otherwise be employed to vaporize the high moisture content in the biomass (Menya et al., 2018; Janković et al., 2019). The presence of ash in a given biomass may be advantageous or problematic to the adsorption process using the resultant AC, depending on its amount in the biomass and subsequently in the resultant AC. For instance, during chemical activation, the activating agent reacts with silica in the ash, reducing the intended optimal activating agent/precursor ratio that is otherwise needed to produce ACs with high adsorption properties (Menya et al., 2018). Aside from this, the high ash content potentially obstructs pore development, leading to AC with relatively low specific surface area (Bandara et al., 2020). To avoid these challenges, the AC precursor should have an ash content of 2%–5% (dried basis) (Serp and Machado, 2015).

High volatile matter content promotes great porosity, and subsequently high surface area of the AC produced (Dzigbor and Chimphango, 2019). Volatile matter content > 70% (dried basis) is desirable for AC production (Janković et al., 2019). However, higher values of volatile matter result in lower fixed carbon values (Olupot et al., 2016) and subsequently lower char and AC yields (Acevedo-Páez et al., 2020). Presence of high amounts of C, H, and O are related to the lignocellulosic composition of the precursor, as well as some minor non-structural components such as proteins, chlorophylls, ash, and waxes (González-García, 2018). In the production of AC, carbon content in the range of 40%–90% is desired for higher char yields (Nieto-Delgado et al., 2011) while low sulfur and nitrogen concentrations of a precursor are preferred to avoid emissions from oxides of these elements during pyrolysis. These oxides are detrimental to the environment (Janković et al., 2019).

### 3.3. Bulk density and hardness

Bulk density and hardness are important parameters to consider when selecting AC precursor materials. These parameters influence the attrition resistance and mechanical strength of the resultant GAC required for application in high pressure aqueous solutions (Smith et al., 2012; Hernández et al., 2014). Resistance to attrition is an important attribute of GAC as it allows maintenance of the physical integrity, as well as withstands the frictional forces during backwashing (Qiu and Guo, 2010). The bulk density also affects the volume that can be handled in the adsorbent unit per unit time (Dzigbor and Chimphango, 2019). On the basis of bulk density, and hardness, coal, peat, wood and coconut based ACs could be used as references in selecting the material suitable for using in continuous columns since these have been widely used in preparation of commercial GAC (Mailler et al., 2016).

## 4. Biomass waste pretreatment

For most lignocellulosic biomass, a pretreatment step may be required to disrupt the recalcitrant structure and subsequently increase the surface area accessible for adsorption (Shahabazuddin et al., 2018). A general pretreatment step that cuts across all biomass wastes as precursors for AC involves size reduction, sieving to preferred particle size, washing and then drying to constant weight (Özdemir et al., 2011; Larous and Meniai, 2012; Bojić et al., 2017; Yu et al., 2020). Washing is done to remove any impurities and soil which might affect the initial properties of the precursor. Sometimes the washing step involves using a known concentration of an acid followed by hot water and then distilled water prior to oven drying of the samples (Bhatnagar et al., 2014). Acid washing removes soluble and insoluble metals, ash and lignin (Crincoli et al., 2020; Kaur et al., 2020), while hot water washing mainly removes the soluble ions from the raw precursor (Bandara et al., 2020). This makes the oxygen functional groups that are key in the adsorption mechanism available (Bojić et al., 2017). The washing efficiency depends on biomass type, particle size, biomass to water/chemical ratio, temperature and washing time (Bandara et al., 2020). Alkaline media like KOH and NaOH react easily with silcon present in some biomass materials such as rice husks, reducing the high ash content of the biomass (Menya et al., 2020). Pretreatment of lignocellulosic biomass with an alkaline expands their internal structure by dissolving some of the lignin which promotes the contact between the precursor and activating agent during activation (Jiang et al., 2020).

From the foregoing discussion, the choice of the pretreatment agent(s), time, and temperature depends on the biomass type and its composition. Water washing is effective for precursors with low ash content (< 10% (dried basis)) with water-soluble minerals

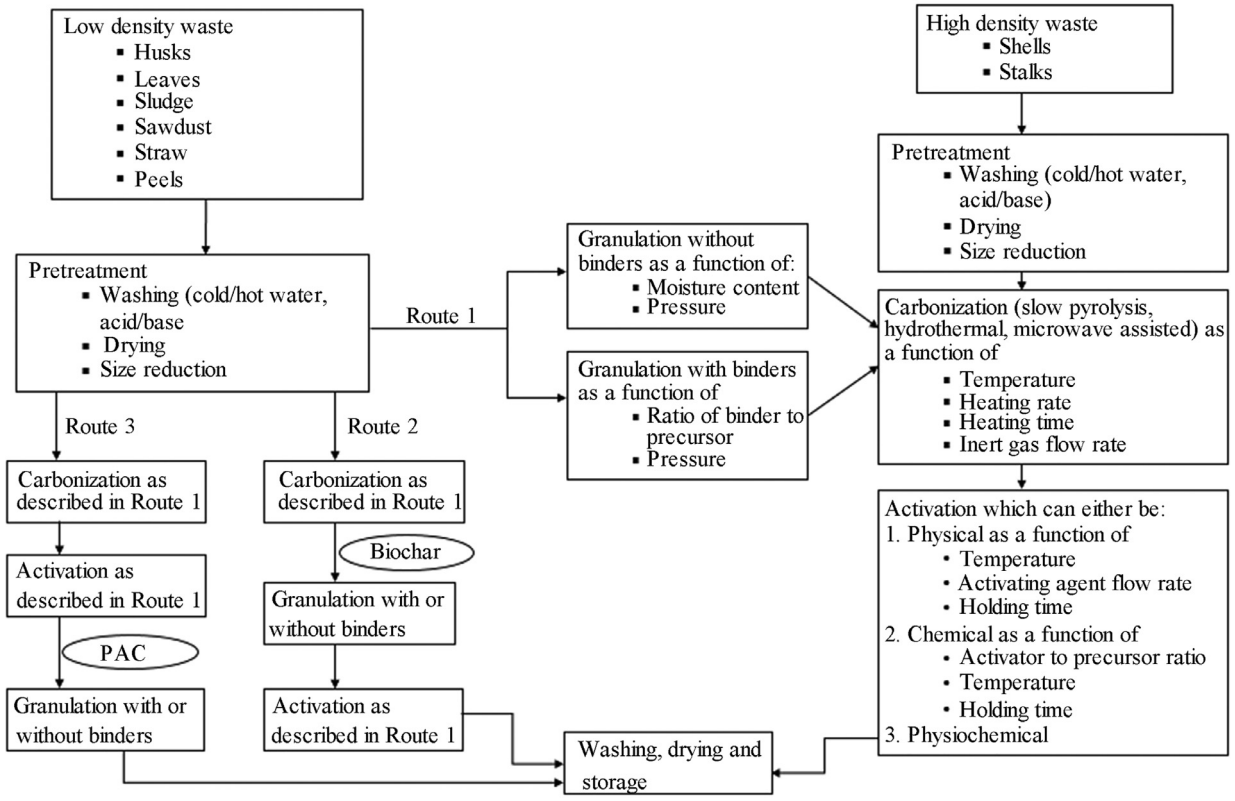


**Fig. 1.** Preparation of granular activated carbon from waste materials using different routes.

in their structure whilst those with ash content greater than 10% (dried basis) may require washing with an acid or a base (Rashidi and Yusup, 2017; Zhang and Chen, 2020). Caution should be taken on how much ash and lignin are removed during pretreatment since this may significantly reduce char and subsequently AC yields. Using hot water could enhance the ash removal from precursors, however, this is offset by the high energy requirements to prepare this water which might not be economically viable especially on large scale production. Much as acids and bases are superior to water in removing ash and promoting adsorptive characteristics, a post washing step is required to remove these chemicals from the pretreated precursor thus making the method costly and liable to pollution.

## 5. Preparation of granular activated carbon

The GAC is preferably derived from hard biomass materials such as the shells from coconut and palm kernel. These shells are activated by physical and/or chemical activation methods to obtain GAC (Fig. 1). The GAC can also be produced through granulation of low density, soft biomass waste materials, as well as through granulation of PAC using binders to produce granules/or pellets with enhanced adsorption properties (Deshannavar et al., 2018). However, in some instances, granulation can also be done without binders (Cai et al., 2018). The challenge associated with the GAC directly derived from biomass waste is its low attrition resistance attributed to the high cellulose content in the biomass waste, which gives it a fibrous and brittle tendency not desired in the production of GACs. This tendency can be reduced through the use of binders (Jaria et al., 2019). The granulation process can be done by spray coating, vibration dropping, extrusion or manually on raw precursors (Mustafa and Asmatulu, 2020), on carbonized precursor (Aransiola et al., 2019; Yu et al., 2020), and/or on PAC (Nagalakshmi et al., 2019; Ghorbani et al., 2020). Granulating the powder-binder mixture and then crushing it to desired particle sizes gives GAC better strength and density than GAC of similar size produced directly without granulation (Yao et al., 2016; Gonçalves et al., 2017). Fig. 1 shows the different pathways that can be employed to prepare GAC from biomass waste materials.

Besides the nature of biomass waste, process parameters also influence the quality of the resultant GAC. Such parameters include mixture ratio (powder to binder ratio), molding pressure, activation temperatures, impregnation order (binder followed by activating agent or vice versa), and activation method. The granulation process, together with its process parameters that influence the quality of the resultant GAC is discussed further in the subsequent sections.

### 5.1. Granulation process

The granulation process involves reduction of biomass to relatively finer particles, which are subsequently squeezed in a press at relatively high pressure, producing granules of a higher density (Guo et al., 2020). Granulation also improves the mechanical strength, structure, and energy density of biomass (Wang et al., 2020b) though granules are more resistant to thermal decomposition than their powder counterparts, thus necessitating a higher activation energy (Guo et al., 2020). Size reduction of biomass to finer particles is also associated with relatively high costs (Wang et al., 2020b).

High granulation pressure increases molecular connections and promotes coherence of adjacent particles in the biomass (Hu et al., 2016). The pressure applied produces heat as a result of friction and softens lignin hence acting as a resin for binding the surface of the granule (Missagia et al., 2011). Biomass with lignin content > 20% (dried basis) can be produced into granules without a binder by utilizing pressures above 150 MPa (Amarasekara et al., 2017). Since the granulation process is closely related to the content of macropores and the hardness of the formed granules, caution should be taken on the amount of pressure applied so that the pores are not completely closed (Dong et al., 2019).

Moisture content (MC) in the range 10%–20% is considered optimal for biomass granulation with lower values leading to disintegration of the granules while higher values reducing the durability and strength (Missagia et al., 2011). Granulating at optimal MC also promotes the bonding character of particles by enhancing van der Waals forces and hydrogen bonds (Rizhikovs et al., 2012; Hu et al., 2016). The MC also influences the optimal granulation pressure, use and/or type of binder, as well as power consumption during granulation (Rizhikovs et al., 2012; Smith et al., 2012).

### 5.2. Granulation with binders

Usually for low density wastes, a suitable binder is mixed with powdered particles to form granules and/or pellets that are carbonized and then activated to produce GAC (Gonçalves et al., 2016). Addition of binders can increase the strength, durability (Rajput et al., 2020), and porous structure of granules (Rizhikovs et al., 2012). Binders occupy the void spaces within the small particles and form solid bridges that become stronger upon drying (Muazu and Stegemann, 2015; Mustafa and Asmatulu, 2020). The enhanced strength of GAC using binders is influenced by the type of activating agent and binder, impregnation ratio between precursor, activating agent and binder, impregnation order (activating agent followed by binder, and vice-versa), and carbonization type (Si et al., 2016; Jaria et al., 2019). Caution should be taken when selecting the type of binder so that adverse environmental effects and high costs are not involved (Si et al., 2016). Inorganic binders (such as bentonite, hydrated lime and silicate) may result in corrosion, emissions, deposit formation, since they are rich in minerals (Iftikhar et al., 2019). Organic binders may create GAC with high *meso/*macro pores after calcination at high temperatures (Kim et al., 2016; Gonçalves et al., 2017) hence favoring adsorption of large molecular contaminants. Granules from organic binders usually have higher volatile matter, fixed carbon, and less ash content than their inorganic counterparts (Hu et al., 2015). However, use of organic binders can distort the structural morphology of the formed GAC due to continuous release of organic carbon during operation hence hampering with adsorption capacities (Ogata et al., 2012). There should be an optimum amount of binder added to obtain GAC with good adsorptive properties. Too much levels of binders could decrease the specific surface area of the carbons (Saeidi and Lotfollahi, 2015; Cai et al., 2018) though mechanical strength was increased (Kim et al., 2016; Seyedein Ghannad and Lotfollahi, 2018). The adsorptive properties of biomass based GAC produced using different binders are summarized in Table 2.

### 5.3. Binderless granulation

Most natural biomass materials have inbuilt binders that are activated with application of pressure and heat (Muazu and Stegemann, 2015). The presence of lignin and hemicellulose in biomass enhances the binding process due to activation of inbuilt mono and oligosaccharides that act as internal binders at elevated temperatures (Ahmad et al., 2013; Iftikhar et al., 2019). Binderless granulation produces GAC that is less cohesive (Gonçalves et al., 2017) with negligible compressive strength and hence can easily disintegrate under using in aqueous solutions (Muazu and Stegemann, 2015).

## 6. Carbonization

Carbonization is the thermal decomposition of carbonaceous materials usually at temperatures below 800 ˚C in an inert environment to eliminate non-carbon species and produce a fixed carbon mass. It is a robust process that degrades organic matter into syngas, bio-oil and bio-char depending on the operation conditions (Shaheen et al., 2019). The process leads to disintegration of biomass leading to increased stability, hydrophobicity (Thakur et al., 2020), and initial development of porosity (Sajjadi et al., 2019) though with relatively lower surface area and pore volume than the subsequent AC (Ouyang et al., 2020; Santoso et al., 2020). For granulated binder-based biomass, carbonization helps in strengthening the powder-binder bond (Tian et al., 2018). Temperature, and heating rate are the most influential factors of carbonization (Pallarés et al., 2018; Wang et al., 2020b) with inert gas flow rate, and residence time playing a significant role (Islam and Rouf, 2013; Colantoni et al., 2016). During carbonization process, oxygen is excluded as practically possible so as to prevent oxidation of biomass as well as limit formation of light gases and water. However, achieving a fully inert environment is difficult in continuous pyrolyzers because the void space in bulk biomass contains air (Kim et al., 2014). Thus, understanding the effect of oxygen on pyrolysis of biomass is important in predicting product properties and yields. Nevertheless, presence of appropriate oxygen in pyrolysis atmosphere is beneficial in increasing the total pore volume and specific

**Table 2**
Granular activated carbon (GAC) derived from a mixture of biomass and binders and the resultant carbon properties.

| Precursor used | Binder used | Waste: binder ratio | Granulation process | Post-granulation treatment | Derived GAC properties | | | | Reference |
|---|---|---|---|---|---|---|---|---|---|
| | | | | | Particle size (mm) | $S_{BET}$ surface area ($m^2/g$) | Total pore volume ($cm^3/g$) | Average pore diameter (nm) | |
| Raw waste paper | Molasses | 16:1 | Mixture stirred for 5 min at 3000 r/min using a vortex mixer. Pellets produced using a hydraulic press at a pressure of 5 t/$cm^2$ for 2 min | Chemically impregnated with $ZnCl_2$ pellets carbonized using slow pyrolysis | – | 1496.97 | 0.455 | – | (Mustafa and Asmatulu, 2020) |
| Raw dewatered Paper mill sludge | Ammonium lignosulfonate | 6:5 | Mixture stirred overnight in a head-over-shaker (80 r/min) and left to dry at room temperature followed by overnight oven-drying at 105 °C. | Dried mixture carbonized and then activated using KOH | 0.5–1.0 | 671 | 0.37 | 1.11 | (Jaria et al., 2019) |
| Raw brewery spent grain | Brewer's surplus yeast | 1:1 | Mixture dried at 105 °C for 2–3 h, press-molded in a stainless-steel using a laboratory press at a pressure of 566 kg/$cm^2$ for 1 min to form briquettes (15 mm diameter × 15 mm height) | Carbonized under slow pyrolysis and physically activated using $CO_2$ | 0.6–2.0 | 353.3 | 0.095 | 1.435 | (Gonçalves et al., 2017) |
| Coffee ground PAC | Calcium-alginate | 1:1 | Equal weight of PAC added into equal weight volume of sodium alginate; mixture stirred for 10 h; homogeneous mixture added to equal weight of calcium chloride to form granules | Product oven-dried at 45 °C for 24 h | 2.03 | 704.23 | 0.293 | 2.20 | (Jung et al., 2016) |
| Raw phoenix tree leaves | Bentonite | 1:1 | Deionized water slowly added into the mixture until a homogeneous paste was formed. The paste was then manually made into granules, and air dried | Carbonized under slow pyrolysis | 5–6 | 166.3 | 0.276 | 1.077 | (Liang et al., 2016) |
| Raw Sugarcane bagasse granules | Molasses | 1:0.5 | Mixture dried at 105 °C for 1 h and press- molded in a stainless-steel cylinder using a laboratory press at a pressure of 850 kg/$cm^2$ for 1 min to form pellets (15 mm diameter × 10 mm height) | Carbonized and activated using $CO_2$ in a single step and then crushed to form granules | 1.0–2.8 | 906.1 | 0.174 | 1.505 | (Gonçalves et al., 2016) |
| Carbonized rice husks | Citric acid | – | Mixture stood for 2 h at 20 °C; followed by drying for 18 h at 120 °C | Activated using ferric chloride solution | 2–4 | 99.32 | 0.332 | – | (Dalai et al., 2015) |
| Raw pine sawdust | Coal tar pitch | 10:2 | Uniaxial compression in a stamping tablet machine | Activated in a single step (carbonization-activation) using $CO_2$ | Pellets (4.1 mm diameter × 3.2 mm height) | 783 | 0.33 | 0.75 | (Plaza et al., 2015) |
| Raw walnut shell | Rapeseed oil cake | 1:1 | Mixture extruded into pellets and dried at 105 °C for 8 h | Carbonized by slow pyrolysis followed by activation with $CO_2$ | – | 1080 | 0.464 | 1.90 | (David and Kopac, 2014) |

(*continued on next page*)

**Table 2** (*continued*)

| Precursor used | Binder used | Waste: binder ratio | Granulation process | Post-granulation treatment | Derived GAC properties | | | | Reference |
|---|---|---|---|---|---|---|---|---|---|
| | | | | | Particle size (mm) | $S_{BET}$ surface area ($m^2/g$) | Total pore volume ($cm^3/g$) | Average pore diameter (nm) | |
| Raw dewatered sewage sludge | Soluble starch | 10:3 | 20 mL of water added to the mixture and extruded to form pellets which were dried at 105 °C for 2 h | Carbonized under slow pyrolysis | Pellets (4 mm diameter × 9 mm height) | 55.60 | 0.043 | 3.12 | (Liu et al., 2014) |
| Raw dewatered sewage sludge | Sodium CMC | 10:3 | 20 mL of water added to the mixture and extruded to form pellets which were dried at 105 °C for 2 h | Carbonized under slow pyrolysis | Pellets (4 mm diameter × 9 mm height) | 39.06 | 0.030 | 3.08 | (Liu et al., 2014) |
| Raw dewatered sewage sludge | Sodium silicate | 10:3 | 20 mL of water added to the mixture and extruded to form pellets which were dried at 105 °C for 2 h | Carbonized under slow pyrolysis | Pellets (4 mm diameter × 9 mm height) | 2.24 | 0.006 | 9.82 | (Liu et al., 2014) |
| Raw dewatered sewage sludge | Calcium sulfate | 10:3 | 20 mL of water added to the mixture and extruded to form pellets which were dried at 105 °C for 2 h | Carbonized under slow pyrolysis | Pellets (4 mm diameter x 9 mm height) | 14.27 | 0.029 | 8.07 | (Liu et al., 2014) |
| Raw dewatered paper mill sludge | Polyvnyl alcohol and CMC | – | Mixture added with 8wt% Bentonite | Carbonized with slow pyrolysis, acid washed, active using steam | 0.4–1.0 | 176 | – | – | (Li et al., 2011) |
| Raw poultry litter | Hydrated chicken fat | – | Extruded into pellets of 5 mm diameter × 0.3 mm length | Carbonized under slow pyrolysis followed by steam activation | 2.59 | 403 | – | – | (Qiu and Guo, 2010) |
| Carbonized rice husks | Beet sugar syrup | 7:3 | Mixture press molded at 54 MPa for 1 min to form pellets followed by drying at 105 °C for 1 h | Carbonized under slow pyrolysis followed by $CO_2$ activation | – | 1027 | 0.68 | – | (Kumagai et al., 2010) |

surface area of biochar (Zhang et al., 2016). Three forms of carbonization commonly employed on biomass wastes are discussed below.

### 6.1. Pyrolysis

Pyrolysis requires a slow heating rate (< 10 °C/min) of biomass at 400–700 °C with residence times of 1–3 h (Ellison et al., 2020; Kwon et al., 2020). The pyrolysis process consists of four stages including: 1) dehydrating of the moistures from waste structures at temperatures below 200 °C, 2) decomposition of biomass with discharge of organic acids and light tars at temperatures of 170–270 °C, 3) further decomposition of biomass at temperatures of 270–350 °C with evolution of significant amounts of liquids and gases leading to formation of biochar, and 4) removal of remaining volatiles with acceleration of carbon formation at temperatures > 350 °C (Rashidi and Yusup, 2017). An increase in temperature leads to a decrease in biochar yield (Rizhikovs et al., 2012; Colantoni et al., 2016; Wang et al., 2020b) due to an increased burn off (Yahya et al., 2015). Temperatures above 600 °C may result into diffusion effects and are thus not normally used (Wang et al., 2020b). In order to obtain low volatilization and high char yields at relatively higher temperatures, low heating rates (10–15 °C/min) are employed (Mohamad Nor et al., 2013). Pyrolysis temperature also affects elemental composition, pore size distribution, pore volume, and surface chemistry of biochar (Ahmad et al., 2013; Colantoni et al., 2016; Shen et al., 2017).

### 6.2. Hydrothermal carbonization (HTC)

The HTC is a method of producing char from aqueous biomass in an autoclave at temperatures below 350 °C with self-generated pressure (2–5 MPa) for several hours (Ouyang et al., 2020; Sharma et al., 2020). It involves a series of chemical reactions such as hydrolysis, dehydration, decarboxylation, aromatization, and re-condensation in the presence of water (Başakçılardan Kabakcı and Baran, 2019). The solid product obtained after HTC is referred to hydrochar. The hydrochar has a high concentration of oxygenated functional groups such as hydroxylic, carboxylic, and phenolic which enhance its hydrophilic properties and the subsequent adsorption capacity (Jain et al., 2015; Benstoem et al., 2018). Hydrochar can easily form granules without use of binders (Wu et al., 2018; Yu et al., 2020). This could be attributed to polar organic compounds such as bio-oil (Song et al., 2020) and hemicellulose autohydrolysis products (Rizhikovs et al., 2012) produced during HTC which act as bridges between particles hence bonding them together.

The performance of HTC in an aqueous phase implies that biomass with high moisture content can easily be carbonized which saves time, energy and cost for drying the precursors (Rashidi and Yusup, 2017). Compared with biochar (char produced by pyrolysis), hydrochars have higher amount of fixed carbon (Shaheen et al., 2019). This is because lignin which is the major contributor to fixed carbon can not be degraded at HTC low temperatures (Başakçılardan Kabakcı and Baran, 2019). Contrary to pyrolysis which increases ash content in biochar, hydrochars have reduced ash content due to biomass demineralization (Missaoui et al., 2017).

### 6.3. Microwave assisted carbonization

Under microwave irradiation, heat is generated by ionic conduction and dipole rotation which rapidly increases the particle temperature. The temperature is uniformly distributed throughout the sample (Hoseinzadeh Hesas et al., 2013). When a high-frequency voltage is given to a sample material, the molecules with permanent dipole moment, align in the direction opposite to that of the applied field leading to generation of heat by dipole–dipole rotation (microwave irradiation) (Pathak and Mandavgane, 2015). Microwave heating is associated with reduced heating time, energy and gas consumption but with even heating of biomass (Hejazifar et al., 2011; Njoku et al., 2013). Microwave irradiation is also associated with selective heating, reduced equipment size, indirect contact between the sample and heating source, and little or no automation (Omorogie et al., 2017). Unlike conventional heating where heat has to be transferred to the particles by conduction or convection radiation, microwave pyrolysis involves heat transfer from the inside to the outside of the particle by irradiation mechanism (Bu et al., 2013; Cheng et al., 2016). The generated volatile matter migrates from high-temperature particle interior to a lower temperature zone in the particle surroundings (An et al., 2020). This thus solves the problem of thermal gradient associated with conventional heating methods hence increasing the char yield (Cheng et al., 2016). In microwave carbonization, biochar yield is mainly influenced by heating rate and radiation power (Ouyang et al., 2020). Microwave HTC could be employed to reduce on the longer holding times involved with oven HTC (Shao et al., 2020). This leads to improved adsorption properties while saving energy. The effects of carbonization type on char yield and its properties are summarized in Table 3.

## 7. Activation

Chars have low porosity and surface area due to formation and condensation of hydrocarbons on their surfaces (Masoumi and Dalai, 2020). Activation process enhances the enlargement of pore diameter and increases the porosity of ACs (Mohamad Nor et al., 2013; Mustafa and Asmatulu, 2020). The activation process involves three major stages namely: 1) elimination of tarry substances that cause pore blockage to enable the elementary carbon crystal surface come into contact with the activating agents, 2) burning of the elementary carbon crystal, and 3) oxidation of the carbon particles (Chowdhury et al., 2013).

The activation step is greatly influenced by temperature and holding time which largely depend on the nature of the precursor, binder, activator used, and target adsorbate (Kalderis et al., 2008b). It is key to select optimal temperature and time that give high specific surface areas, sufficient pore development, and surface functional groups without diminishing the mechanical strength of the

**Table 3**
Char yield and properties obtained from different biomass wastes employing either pyrolysis, hydrothermal carbonization or microwave assisted carbonization.

| Precursor and its pre-carbonization state | Precursor particle size (mm) | Optimal carbonization condition | Char yield (%) | Char property | | | Reference |
|---|---|---|---|---|---|---|---|
| | | | | Surface area ($S_{BET}$, $m^2/g$) | Total pore volume ($cm^3/g$) | Average pore diameter (nm) | |
| Pyrolysis | | | | | | | |
| Raw pineapple peels | 1 | Heated and maintained at 550 °C for 1 h at 5 °C/min under $N_2$ flow | 32.08 | 11.11 | 0.017 | 3.11 | (Shakya and Agarwal, 2019) |
| Raw durian shell | 1–2 | Heated to 700 °C, at 10 °C/min under $N_2$ flow (150 $cm^3$/min) | – | 8.41 | 0.011 | 2.331 | (Foo and Hameed, 2012a) |
| Raw grape waste | – | Heated and maintained at 600 °C for 1 h at 10 °C/min under $N_2$ flow (100 mL/min) | – | 6.73 | 0.013 | 7.84 | (Sayğılı et al., 2015) |
| Raw pecan shell | 0.8 | Heated and maintained at 700 °C for 2 h at 10 °C/min under $N_2$ flow | 36.34 | 331 | 0.171 | 1.956 | (Aguayo-Villarreal et al., 2017) |
| Raw spent coffee ground | 0.15 | Heated to and maintained at 500 °C for 2 h at 10 °C/min under $N_2$ flow (0.25 L/min) | – | 11.0 | 0.009 | | (Shin et al., 2020) |
| Acid pretreated Boabab seed | 3 | Heated to 900 °C at 10 °C/min under $N_2$ flow (85 $cm^3$/min) | 28.2 | 319 | 0.28 | 3.52 | (Tchikuala et al., 2017) |
| Raw avocado kernel seeds | 0.672 | Heated and maintained at 800 °C for 2 h at 10 °C/min under $N_2$ flow (294 mL/min) | 21.85 | 52.4 | 0.051 | 0.94 | (Salomón-Negrete et al., 2018) |
| Raw wheat straw | 1 | Heated and maintained at 600 °C for 1 h at 2 °C/min under $N_2$ flow (100 mL/min) | – | 6.89 | 0.007 | – | (Cao et al., 2019) |
| Raw apricot kernel shell | 1 | Heating from 25 °C to 850 °C at 4 °C/min ad held at 850 °C for 1 h at $N_2$ flow rate of 500 $cm^3$/min | – | 328.570 | – | – | (Janković et al., 2019) |
| Raw peanut shell | 0.2–2.5 | Heated to and held at 600 °C for 1 h at 50 °C/min under $N_2$ flow (5 L/min) | 32.21 | 1.7 | 0.20 | – | (Mohammed et al., 2016) |
| Hydrothermal | | | | | | | |
| Raw microalgae | 1.18 | Temperature 222 °C, Pressure 11.5 MPa for 15 min | 75.6 | 366 | 0.2 | 5.6 | (Masoumi and Dalai, 2020) |
| Raw pine sawdust | 0.22–0.49 | The 9 g of sawdust mixed with 150 mL of DI water, mixture heated at 220 °C for 30 min under Ar flow | 64.01 | 2.62 | 0.019 | 9.48 | (Huang et al., 2019) |
| Raw wastewater sludge (88.86% moisture content | – | Heated and maintained at 260 °C for 1 h at 20 °C/min to form a solid product | 31.08 | 6.2 | 0.015 | 2.95 | (Khoshbouy et al., 2019) |
| Raw olive pomace | 0.25 | Heated at 220 °C for 90 min | 65.8 | 473.8 | 0.25 | 1.05 | (Başakçılardan Kabakcı and Baran, 2019) |

(*continued on next page*)

**Table 3** (*continued*)

| Precursor and its pre-carbonization state | Precursor particle size (mm) | Optimal carbonization condition | Char yield (%) | Char property | | | Reference |
|---|---|---|---|---|---|---|---|
| | | | | Surface area ($S_{BET}$, $m^2/g$) | Total pore volume ($cm^3/g$) | Average pore diameter (nm) | |
| Raw walnut shell | 0.25 | Heated at 220 °C for 90 min | 64.8 | 642.6 | 0.35 | 1.08 | (Başakçılardan Kabakcı and Baran, 2019) |
| Raw tea stalk | 0.25 | Heated at 220 °C for 90 min | 71 | 666.7 | 0.36 | 1.08 | (Başakçılardan Kabakcı and Baran, 2019) |
| Hazelnut husk | 0.25 | Heated at 220 °C for 90 min | 65.8 | 631.3 | 0.39 | 1.25 | (Başakçılardan Kabakcı and Baran, 2019) |
| Raw corn stalk | < 0.18 | Heated at 150 °C for 15 min at 5 g corn stalk per 50 mL $H_2O$ | 73.94 | 2.14 | 0.01 | 12.04 | (Kang et al., 2019) |
| Microwave assisted carbonization | | | | | | | |
| Raw rice husk | – | Microwave power 900 W, radiation time 15 min, temperature 600 °C, $N_2$ flow (0.2 L/min) | 39 | 190 | – | 3.496 | (Shukla et al., 2019) |
| Chemically impregnated pine sawdust | 0.3 | Microwave power 600 W; radiation time 30 min | 34.82 | 304.49 | 0.149 | 3.92 | (Omorogie et al., 2017) |
| Chemically impregnated walnut shell | 2 | Microwave power 800 W; radiation time 20 min under $N_2$ flow | – | 418 | 0.35 | | (Duan et al., 2017) |
| Chemically impregnated mushroom roots | 0.15–0.25 | Radiation power 800 W; radiation time 15 min | 52.6 | 1024 | 0.891 | 3.24 | (Cheng et al., 2016) |
| Chemically impregnated Sapelli wood chips | 0.3 | Microwave power 600 W; radiation time 11 min under $N_2$ flow (200 mL/min) | – | 90.5 | 0.026 | | (Thue et al., 2016) |
| Chemically impregnated grapevine shoots | 0.6–0.84 | Microwave power 400 W; radiation time 2 min | – | 1607 | 1.42 | 3.53 | (Hejazifar et al., 2011) |

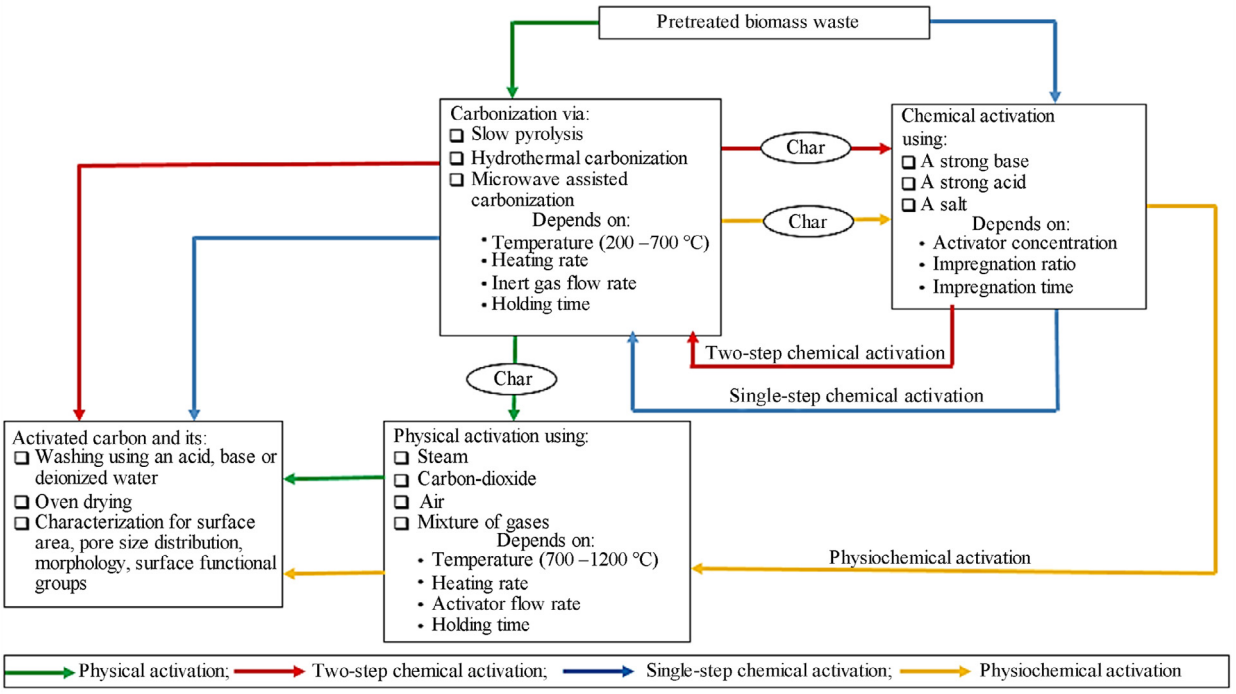


**Fig. 2.** A schematic of physical, chemical and physiochemical activation of biomass wastes.

AC (Dong et al., 2018; Bhomick et al., 2019). Low activation temperature and time lead to poor development of surface area due to reduction in volatilization of organics (Yu et al., 2020). High temperatures lead to expansion of pores due to material decomposition (Yagmur et al., 2020). Increase of activation temperature increases the rate of reaction between the activator and the precursor which in turn leads to formation of greater micropores that have a great influence on specific surface areas (Cao et al., 2006). There is a temperature limit after which further increases might affect the surface properties of the carbon (Chowdhury et al., 2013). Much as activating at high temperatures under $N_2$ flow increases the surface functionality of the carbon adsorbent (Santoso et al., 2020) and hence the adsorption capacity (Tran et al., 2019), very high temperatures could lead to pore shrinkage due to structural destruction and oxidation of carbon frameworks which reduces specific surface area (Lee et al., 2018).

Shorter activation time does not enable formation of micro and mesopores (Bae et al., 2014) while longer times destroy these pores due to the collapse of carbon structure and pore wall destruction (Lee et al., 2018). The destruction of the pores at longer activation times is attributed to gasification of the already developed micropore walls (Islam and Rouf, 2013). Two methods of activation namely; physical, and chemical are used in production of ACs (Fig. 2). Sometimes the two methods can be combined to form a physiochemical activation method.

### *7.1. Physical activation*

Physical activation is a two-stage process that involves carbonization followed by activation in presence of an oxidizing agent such as steam, carbon-dioxide, air or a mixture of them at high temperatures (Fig. 2). The choice of the activating agent affects surface properties and porosity of the formed carbons. Carbon-dioxide is a preferred agent since it is a clean gas with low reaction rate at activing temperatures which makes its handling easy (Rashidi and Yusup, 2017). Carbon-dioxide also gives rise to both higher carbon yields and higher levels of microporosity as compared to steam. Lower AC yield by steam activation could be attributed to rapid material degradation by water molecules at high temperatures (Zaini et al., 2021). However, on the basis of higher surface area and pore volume, steam is a better activating agent than $CO_2$. This is because the adsorption and desorption of moisture occur spontaneously on the active site of biochar to form hydrogen and oxygen containing groups that enhance the surface area and pore formation (Ouyang et al., 2020). Water molecules also diffuse faster and react into the surface of carbon as compared to $CO_2$ (Menya et al., 2018). Nevertheless, there are some cases where biomass waste activated with $CO_2$ has shown better surface area and pore volume than that of steam (Aworn et al., 2008; Pallarés et al., 2018). The choice of steam or $CO_2$ for larger surface areas and pore volumes could thus depend on the raw material being activated. High density materials like shells and seeds are better activated with steam while fibrous and low density materials like straws and husks are better suited for $CO_2$ activation (Aworn et al., 2008). Although there exists a positive correlation between adsorption capacity of the carbon and the developed surface area, some carbons with high surface areas show low adsorption capacities (Santoso et al., 2020). This difference is caused by the molecular size of the target pollutant, solution pH and presence of different functional groups of the carbon surface among other factors.

### 7.2. Chemical activation

Chemical activation as illustrated in Fig. 2, involves an impregnation step where the material either in its raw or carbonized form is mixed with a chemical and then activated. It can be a single step when the raw precursor is mixed with the activating agent and then carbonized or a two-step when the carbonized precursor is mixed with the activating agent and then carbonized (Fig. 2). The activating agent can be a strong base, an acid or a salt. The common activating agents are: $H_2SO_4$, $H_3PO_4$, NaOH, KOH, HCl, $ZnCl_2$, $CaCl_2$, and HF. Strong bases such as KOH are usually employed in single step activation (Masoumi and Dalai, 2020). Activating with $H_3PO_4$ yields carbons with low surface areas due to creation of phosphate esters and their high retention in the solid carbon matrix (Kalderis et al., 2008a). The $ZnCl_2$ is usually employed to produce AC with relatively high surface area and porosity because it is a Lewis acid having only a dehydrating role in producing AC and hence does not react with carbon (Sayğılı et al., 2015; Ouyang et al., 2020). The two step activation enables the activating agent to diffuse into the pores and react with the carbon easily hence creating more pores (Chowdhury et al., 2013). Carbonization temperatures are usually lower than activation temperatures in a two-step chemical activation process (Fu et al., 2018). The choice of the material state (raw vs. carbonized) and the activating agent affects the final morphology and hence the adsorption properties of the derived carbons.

Chemical activation is greatly influenced by the impregnation ratio of the activator to the precursor. The impregnation ratio affects the developed surface area, carbon yield, adsorption capacity and activation energy. Use of excess activator could reduce the specific surface area due to higher extent of chemical reaction leading to destruction of pores (Masoumi and Dalai, 2020). The excess activator enlarges the volume of the pores and causes extra carbon burn off which in turn affects the adsorption capacity of the carbons (Foo and Hameed, 2012a). Excess activator can restrict the release of any liquids and tars. This in turn blocks pore passages of the carbon surface during activation (Hoseinzadeh Hesas et al., 2013). Increasing the mass ratio of the activator to precursor also reduces the activation energy (Fu et al., 2018). The impregnation of the activator and the precursor can either be dry or wet (Rashidi and Yusup, 2017). In dry impregnation, the powdered activating agent is directly mixed with the precursor (raw or char) followed by a thermal treatment method. On the other hand, wet impregnation involves adding the precursor to a solution of water and activating agent followed by continuous stirring. Dry mixing produces ACs with better adsorption properties in terms of surface area and pore volume as compared to wet mixing (Kan et al., 2015).

Both chemical and physical activation methods can be combined to form a physicochemical activation process. This involves carbonization of a chemically impregnated raw precursor followed by physical activation or the carbonization and activation of chemically impregnated char with oxidizing gas or steam (Fig. 2). The method is employed in a post-carbonization stage where the chemical agents were not fully eliminated even after washing which could inhibit pore formation (Ao et al., 2018).

### 7.3. Comparison among physical, chemical, and physiochemical activation

Selection of the activation method depends on the nature of the precursor, and the intended use of the derived AC (Hoseinzadeh Hesas et al., 2013). At an industrial scale, physical activation is preferred because it allows for the optimization of the pyrolysis stage by enabling a greater control over micro-porosity development (Pallarés et al., 2018). In addition, ACs produced by physical activation do not require chemical neutralization especially for carbons to be used in water treatment thus reducing both the process costs and associated pollution. Physically ACs are also associated with higher physical strength which favors their use in high pressure columns (Yang et al., 2010). These factors could thus explain why most GAC used in water treatment are prepared via physical activation.

The advantages of chemical activation over physical activation lie in the lower activation temperature, shorter treatment time, reduced energy requirements, and greater AC yield with a larger surface area and pore volume (Supong et al., 2019). However, this comes at the expense of higher process and chemical costs (Bergna et al., 2020). The higher carbon yields of chemical activation method are due to the combined effect of lower activation temperatures and dehydrating effect of the agents that inhibit the formation of tar. For chemical activation, the internal micro-pores are homogeneously developed without significant morphological changes as opposed to physical activation. It is this non-homogeneity in shape and pore development that leads to higher weight losses and hence lower yields by physical activation (Ideta et al., 2020). The physiochemical activation method produces carbons with higher specific surface area, and pore volume than the individual activation methods due to improved mass transfer within the carbon matrix (Chowdhury et al., 2013; Aguayo-Villarreal et al., 2017) and thus, these carbons have a superior adsorption capacity. The optimal conditions for preparation of biomass based GAC using either physical, chemical or physio-chemical activation are shown in Table 4.

## 8. Use of GAC for water treatment

Water treatment involves the removal of pollutants from water with treatment processes based on the type, and concentration of the target pollutant. The most common water treatment processes used worldwide are desalination, filtration, adsorption, biological/chemical membranes, sedimentation, coagulation-flocculation, and aeration (Mustafa and Asmatulu, 2020). Among these, sedimentation, flocculation and filtration are frequently used when only physical particles are to be removed while for dissolved organic and inorganic materials, aeration, desalination, chemically activated membranes, and adsorption are recommended (Mustafa and Asmatulu, 2020). Adsorption of contaminants by GAC is highly utilized as a polishing step in drinking water production (Jusoh et al., 2011; Piai et al., 2020) due to high efficiency, simple operation and flexible design of the technology (Seyedein Ghannad and Lotfollahi, 2018). In advanced water treatment plants where high quality is desired, GAC is integrated with other treatment processes such as ozonation (Popov et al., 2020), oxidation (Crincoli et al., 2020), ultrafiltration membranes (Huang et al., 2020), coagulation-sedimentation-filtration (Hu et al., 2018), and slow sand filters (Paredes et al., 2016).

**Table 4**
Preparation of Granular activated carbon (GAC) from biomass wastes using either physical, chemical or physiochemical activation method and properties of derived carbon.

| Pre-activation state of precursor | Precursor particle size (mm) | Optimal activation condition | Activated carbon yield (%) | GAC property | | | Reference |
|---|---|---|---|---|---|---|---|
| | | | | $S_{BET}$ surface area ($m^2/g$) | Total pore volume ($cm^3/g$) | Average Pore diameter (nm) | |
| Physical activation | | | | | | | |
| Carbonized avocado kernel seeds | 0.672 | Activated and maintained at 1000 °C for 2 h under $CO_2$ flow (147 mL/min) | 11.60 | 299.9 | 0.172 | 0.67 | (Salomón-Negrete et al., 2018) |
| Acid pretreated carbonized Baobab seeds | 3 | Activated up to 850 °C under $CO_2$ (75 mL/min) | 38 | 2130 | 1.74 | 1.94 | (Tchikuala et al., 2017) |
| Carbonized pellets produced from sugarcane bagasse/molasses mixture | – | Activated up to 900 °C under $CO_2$ (83 $cm^3$/min) for 4 h and later ground to form GAC of 1.0–2.8 mm | 17.5 | 906.10 | 0.174 | 1.505 | (Gonçalves et al., 2016) |
| Carbonized briquettes produced from brewery spent grain/brewer yeast mixture | – | Heated at a rate of 10 °C/min under $N_2$ flow (150 mL/min) until it reached 850 °C. At this point, the gas flow was changed to $CO_2$ (100 mL/min) and the samples activated for 2 h and later ground to form GAC of 0.6–2.0 mm | 17.17 | 353.3 | 0.095 | 1.435 | (Gonçalves et al., 2017) |
| Raw pine saw dust pellets | | Equal mix of $CO_2$ and $N_2$ at a flow rate of 100 $cm^3$/min. Heated up to 800 °C for 2 h at 5 °C/min | 40 | 281 | 0.24 | 0.74 | (Plaza et al., 2015) |
| Carbonized pellets produced from walnut shell/rape seed oil cake mixture | | The 65% $CO_2$ in $N_2$ at flow rate of 30 mL/s. Heated and maintained at 750 °C for 3 h at 5 °C/min | 31.05 | 1080 | 0.464 | 1.90 | (David and Kopac, 2014) |
| Hydrochar grey alder wood granules | 1–3 | Activated up to 850 °C at 20 °C/min under superheated steam for 90 min at stem/char ratio of 3:1 | 18.2 | 1338 | 0.88 | 2.63 | (Rizhikovs et al., 2012) |
| Carbonized Macadamia nut shells | 1–2 | Activation temperature 1000 °C under $CO_2$ gas | 32 | 602 | 0.402 | 1.77 | (Poinern et al., 2011) |
| Carbonized Poultry litter granules | 2.59 | Activated up to 700 °C under steam (2.5 mL/min) for 45 min | 31.3 | 403 | – | – | (Qiu and Guo, 2010) |
| Chemical activation | | | | | | | |
| Hydrochar Microalgae | 1.18 | The KOH/hydrochar impregnation ratio, 1.5; activation temperature, 675 °C; $N_2$ flow rate, 267 $cm^3$/min | 61.3 | 2099 | 1.2 | 5.9 | (Masoumi and Dalai, 2020) |
| Carbonized date press cake | 0.5–1.0 | The NaOH/precursor impregnation ratio 2:1 all at 650 °C. under $N_2$ flow (100 mL/min), heating rate of 20 °C/min, for 2 h | 26.2 | 2025.9 | 0.932 | 1.839 | (Norouzi et al., 2018) |
| Raw Peanut shell | 0.833–1.651 | The 88% $H_3PO_4$; acid/precursor impregnation ratio, 1.5; heated at 10 °C up to 650 °C and maintained at this temperature for 2 h under $N_2$ flow (100 mL/min) | 37.2 | 965.678 | – | – | (Garg et al., 2019) |
| Raw orange peels | 5 | The $ZnCl_2$/precursor impregnation ratio of 1:1. mixture dried at 110 °C then heated and held 500 °C for 1 h at 10 °C/min under $N_2$ flow (100 mL/min) | 37 | 1215 | 0.68 | 2.2 | (Köseoğlu and Akmil-Başar, 2015) |
| Raw Palm shell | 0.4–2.5 | The $ZnCl_2$/precursor impregnation ratio of 1.65 microwave power, 1200 W; activation time, 15 min | 54.82 | 1253.5 | 0.83 | 2.65 | (Hoseinzadeh Hesas et al., 2013) |
| Raw *Parkinsonia aculeata* sawdust | 0.75–1.50 | The 50% $H_3PO_4$; acid/precursor impregnation of 2; mixture dried at 110 °C for 2 h; then heated under self-generated atmosphere at 3 °C/min up to 450 °C and held at 0.5 h | 47.0 | 968 | 0.70 | 2.9 | (Nunell et al., 2012) |
| Carbonized *Parkinsonia aculeata* sawdust | 0.75–1.50 | The KOH at KOH/char impregnation ratio of 1; mixture heated to 300 °C at 10 °C/min for 2 h under $N_2$ flow (150 $cm^3$/min); raising the temperature to 800 °C at same heating rate and gas flow for 2 h | 19.8 | 768 | 0.37 | 1.9 | (Nunell et al., 2012) |

(*continued on next page*)

**Table 4** (*continued*)

| Pre-activation state of precursor | Precursor particle size (mm) | Optimal activation condition | Activated carbon yield (%) | GAC property | | | Reference |
|---|---|---|---|---|---|---|---|
| | | | | $S_{BET}$ surface area ($m^2/g$) | Total pore volume ($cm^3/g$) | Average Pore diameter (nm) | |
| Carbonized Durian shell | 1–2 | The NaOH at NaOH/char impregnation ratio of 1.5; microwave radiation power, 600 W; time, 5 min | 87.38 | 1475.48 | 0.841 | 2.281 | (Foo and Hameed, 2012a) |
| Grape vine shoot | – | The 85wt% $H_3PO_4$; acid/precursor impregnation ratio, 5:130:1; impregnation time, 24 h; heating time, 7 h | – | 1607 | 1.42 | 0.28 | (Hejazifar et al., 2011) |
| Carbonized sunflower seed hull | 1–2 | The $K_2CO_3$; at $K_2CO_3$/char impregnation ratio of 1:1.15; microwave power, 600 W, irradiation time, 8 min | – | 1411.55 | 0.836 | 2.361. | (Foo and Hameed, 2011) |
| Carbonized Pineapple peels | 1–2 | The KOH at char/activator ratio of 1:1.25; activated under microwave, 600 W for 6 min; under $N_2$ flow (300 $cm^3$/min) | – | 1006 | 0.59 | 2.34 | (Foo and Hameed, 2012b) |
| Raw olive waste cake | 1.5 | The $H_3PO_4$, 60wt% concentration; acid/precursor impregnation ratio, 1.75 agitated for 2 h at 104 °C; subjected to pyrolysis 450 °C for 2 h under $N_2$ flow (0.5 L/min) | – | 793 | 0.49 | 4.2 | (Baccar et al., 2010) |
| Physiochemical activation | | | | | | | |
| Raw Pecan shell | 0.8 | Chemical: 1 g of precursor mixed in 5 mL of 0.5 mol/L of KCl, mixture heated at and maintained 700 °C at 10 °C/min under $N_2$ flow<br>Physical: chemically activated precursor heated to 700 °C at 10 °C/min under $CO_2$ for 2 h. | 26.14 | 808 | 0.546 | 2.672 | (Aguayo-Villarreal et al., 2017) |
| Raw Oil palm shell | 2–3 | Chemical: 43% KOH; KOH/precursor impregnation ratio of 2:1; heated at 800 °C for 2 h at 5 °C/min under $N_2$ flow (150 $cm^3$/min)<br>Physical: chemically activated precursor heated at temperatures of 800 °C at 5 °C/min under $CO_2$ flow for 1.5 h | 21 | 1614 | 0.57 | 2.2 | (Hamad, 2015) |
| Carbonized Palm oil fronds | 1.5 | Chemical: KOH/char impregnation ratio of 3.75; mixture dehydrated overnight at 100 °C<br>Physical: chemically activated precursor heated and maintained at 750 °C for 3 h at 10 °C/min under $CO_2$ | 20.5 | 1237.13 | 0.667 | 2.16 | (Salman, 2014) |
| Carbonized Palm empty fruit bunch | – | Chemical: KOH/char impregnation ratio of 1:1; mixture dehydrated for 2 h at 85 °C<br>Physical: chemically activated precursor heated to 800 °C at 10 °C/min under $CO_2$ (100 $cm^3$/min) | – | 720.00 | 0.34 | 1.889 | (Nasri et al., 2013) |
| Raw Palm shell | 1–2 | Chemical: 85% $H_2PO_3$; acid/precursor impregnation ratio of 9.42; heated at 405 °C for 2 h at 5 °C/min under $N_2$ flow (100 mL/min)<br>Physical: chemically activated precursor heated at temperatures of 855 °C at 10 °C under $CO_2$ flow for 135 min | – | 642 | 0.28 | 1.766 | (Arami-Niya et al., 2012) |
| Raw Cotton stalk | 3.35–4.75 | Chemical: 50% $ZnCl_2$; 4 g of precursor impregnated in $ZnCl_2$ for 72 h<br>Physical: chemically impregnated precursor carbonized at 900 °C under $N_2$ flow (100 $cm^3$/min) at 10 °C/min, at 900 °C flow changed $CO_2$ for 30 min | – | 2053 | 1.973 | – | (Özdemir et al., 2011) |
| Raw Coffee residue | 1–2 | Chemical: KOH/precursor impregnation ratio 3:1 oven dried at 105 °C for 24 h<br>Physical: chemically activated precursor heated to 700 °C at 10 °C/min under $N_2$ flow and gas changed to $CO_2$ after attaining 700 °C for 3 h | – | 1053 | 1.23 | – | (Giraldo and Moreno-Piraján, 2012) |

### 8.1. Major pollutants in water and their removal by GAC

Water contains various types of contaminants such as pesticides, heavy metals, total dissolved solids, colour, odour, natural organic matter (NOM), microbial contaminants, pharmaceuticals, personal care products (PCPs), disinfection byproducts (DBPs), nitrates, endocrine disrupting chemicals (EDCs), chelating agents, dyes, among others. Discussing all these contaminants is not feasible in this review due to differences in their characteristics, negative effects to the environment and human health, their removal mechanisms and above all the need to limit the length of this manuscript. Attention is briefly given to contaminants of emerging concerns such as pesticides, surfactants, pharmaceuticals, PCPs, EDCs, NOM, DBPs and microplastics. Contaminants of emerging concern (CECs) are anthropogenic or naturally occurring chemicals or microorganisms not routinely monitored but may pose a significant risk due to their potential toxicological effects when present in water bodies (Nawaz and Sengupta, 2019; Pesqueira et al., 2020). The removal of most CECs by physical processes such as sedimentation and flocculation is not feasible owing to the polar or semi polar nature of these contaminants that makes their solubility in water high (Ahmed et al., 2017). Methods used with their associated advantages and drawbacks in removing CECs from aquatic solutions have been discussed in details by Ahmed et al. (2017). Among these methods, membrane bioreactors, activated sludge and aeration have shown good removal efficiencies towards EDCs, PCPs and surfactants while pesticides and pharmaceuticals have been efficiently removed by GAC (Ahmed et al., 2017). The proceeding discussion thus outlines the potential of GAC in removing some key CECs from aquatic solutions.

#### 8.1.1. Natural organic matter

Natural organic matter (NOM) refers to all organic compounds in particulate or dissolved forms, except synthetic molecules such as organic micro pollutants, present in terrestrial or aquatic environments (Levchuk et al., 2018). Presence of NOM in water affects the performance of water treatment processes and the quality of water (Velten et al., 2011). For example, NOM influences odor and taste and it can become a carrier for toxic contaminants contributing to biofilm formation and bacterial regrowth in water distribution systems (Wang et al., 2017). Furthermore, NOM can react with chlorine in drinking water to form halogenated DBPs (Sindelar et al., 2014; Park et al., 2019). The NOM exists in water as hydrophilic and hydrophobic components. The hydrophilic NOM which has a low molecular weight is rich in nitrogenous compounds (such as proteins, amino acids and sugars) and aliphatic carbon (Bhatnagar and Sillanpää, 2017). On the other hand, the hydrophobic fraction which comprises of humic substances, hydrocarbons/tannins, and aromatic carbons/amines (Korotta-Gamage and Sathasivan, 2017; Levchuk et al., 2018) has a high molecular weight made of conjugated double bonds and phenolic structures (Bhatnagar and Sillanpää, 2017). The humic substances constitute the major fraction of aquatic NOM, accounting for more than 50% of dissolved organic carbon in water (Matilainen et al., 2011).

Conventionally, NOM is removed by GAC prior to disinfection (Jiang and Zhang, 2018; Levchuk et al., 2018). The rate and extent of NOM adsorption onto GAC filters depend on molecular weight distribution, charge distribution, degree of hydrophobicity, ability to form hydrogen bonds with the GAC surface, physical and chemical characteristics of GAC, among other factors (Velten et al., 2011). The useful GAC pore size range for NOM removal is reportedly the micropores (1–2 nm) and the mesopores (2–50 nm), with pores smaller than 1 nm offering negligible adsorption (Velten et al., 2011). During adsorption of NOM by GAC, a major fraction containing humic substances (which have relatively high molecular weights and sizes) may block mesopores or micropores resulting in rapid saturation of GAC thus preventing other compounds from accessing the adsorbent (Jiang and Zhang, 2018; Golea et al., 2020). The high molecular weight hydrophobic NOM fraction is readily removed by conventional coagulation, such that the influent NOM to GAC treatment stage is dominated by the low molecular fractions (Matilainen et al., 2006).

Although the low molecular weight NOM fractions have access to a larger percentage of the GAC pore volume, and thus could be easily removed based on size considerations, these compounds may also be relatively hydrophilic and, hence, less adsorbable (Velten et al., 2011). This implies that the low molecular hydrophilic fractions pose the greatest removal challenge by GAC and may still present high DBP problems (Golea et al., 2017). This can be solved by running GAC in a biologically active mode, combining both biosorption and biodegradation functions (Fu et al., 2017a). The structural integration of the GAC adsorption sites, and thickness of the biofilms play a crucial role in removing dissolved organic carbon (DOC), NOM, and other DBP precursors as well as increasing the shelf life of GAC (Islam et al., 2020).

#### 8.1.2. Disinfection by-products

Disinfection by-products (DBPs) are the unintended result of destroying harmful pathogens in drinking water by the reactions of disinfectants (chlorine, ozone, chloramines, chlorine-dioxide, UV) with NOM, bromide, and iodide (Nawaz and Sengupta, 2019). The four commonly detected groups of DBPs are haloacetic acids (HAAs), trihalomethanes (THMs), bromate, and chlorite (Palansooriya et al., 2020). Among these, the HAAs and THMs are the mostly studied DBPs due to their presence in high mass concentrations (Golea et al., 2017). Much as over 700 DBPs are in existence, only 11 of these (including four THMs, five HAAs, chlorite, and bromate), are regulated by the United States Environmental Protection Agency (Nawaz and Sengupta, 2019; Verdugo et al., 2020). There are 74 DBPs that have been categorized as CECs based on their occurrence and toxicity levels (Islam et al., 2020). The detrimental effects of DBPs to human health can be genotoxic, cytotoxic, mutagenic, carcinogenic, teratogenic, endocrine disrupting, among others as discussed by Sun et al. (2019). The GAC adsorption has been reported as one of the best technologies to control DBPs precursors (Chili et al., 2012; Jiang et al., 2017). The D/DBP rule has described GAC as a suitable technique for controlling DBP through removing DOC, lowering HAA levels and removing some of the ozonation by-products (Islam et al., 2020).

The GAC media properties, its position in the treatment scheme and the characteristics of DBPs precursors all influence the adsorption efficiency (Valdivia-Garcia et al., 2016). The removal efficiency can be improved by shifting the adsorption target of GAC from NOM to intermediate DBPs which have relatively small sizes (Jiang and Zhang, 2018). Chlorinating raw/coagulated water

followed by adsorption with GAC is reported to be more effective in removing DBPs as compared to the traditional method of chlorinating the GAC treated water (Jiang and Zhang, 2018).

#### 8.1.3. Pesticides

Pesticides are products intended to prevent harm caused by pests. Pesticides can be referred to as herbicides, fungicides, bactericides, insecticides, algaecides, avicides, antimicrobials, miticides, nematicides, rodenticides, defoliants, virucides (Foo and Hameed, 2010; Chavoshani et al., 2020) depending on chemical and physical properties, chemical group, mode of application and targeted pest (Alves et al., 2019; Taylor et al., 2020). Pesticides account for the largest amount of chemical substances intentionally released in the environment (Matsushita et al., 2018) and they enter aquatic systems through runoff, spray drift and drainage water (Dong et al., 2021). The adverse effects of pesticides on the human respiratory, circulatory, reproductive, endocrine and regulatory systems are discussed in detail by Chavoshani et al. (2020).

Removal of pesticides in aqueous solution by AC adsorption is reported to be superior to coagulation-sedimentation as well as ozonation (Matsushita et al., 2018). The presence of resilient functional groups like phosphates, chloride, nitrites, and the absence of chromophore in pesticides makes their removal by conventional water treatment methods acute (Debnath et al., 2019). On the other hand, AC exhibits enhanced mass transfer, charged interactions, electron-hole separation, and material anchorage better suited for pesticides adsorption (Debnath et al., 2019). The adsorption of pesticide particles onto GAC is largely governed by molecular size and hydrophobic interactions with partial contribution of $\pi$-$\pi$ electron donor-acceptor interactions between the graphene surface of AC and the adsorbates (Matsushita et al., 2018).

#### 8.1.4. Pharmaceuticals

Pharmaceuticals are products with intended medical purposes or health care for humans and/or animals (Yang et al., 2017). They are discharged to aquatic environments through domestic wastewater, improper manufacturer disposal, hospital discharges, water treatment plants, and sewage treatment with their concentrations ranging from μg/L to ng/L (Yang et al., 2017). The main groups of pharmaceutical pollutants in water include antibiotics, antidepressants, non-steroidal anti-inflammatory drugs, lipid regulators, beta-blockers, diuretics, anti-diabetics, anti-epileptics, and hormones (Ahmed et al., 2017; Ouyang et al., 2020). Pharmaceuticals account for a great proportion of total detectable organic pollutants in surface water, reclaimed water and domestic wastewater (Tang et al., 2020). The removal of pharmaceuticals is influenced by molecular size, hydrophobicity, charge, polarizability and functional groups (Tang et al., 2020). Possible mechanisms for pharmaceuticals removal include hydrophobic interactions, electrostatic interactions, hydrogen bonding, $\pi$-$\pi$ interaction/stacking among others (Jin et al., 2020).

#### 8.1.5. Microplastics

Microplastics (MPs) are plastic particles with sizes less than 5 mm (Nawaz and Sengupta, 2019; Shruti et al., 2020) while those < 100 nm are referred to as nanoplastics (Novotna et al., 2019). The MPs result from degradation of bigger plastic materials that enter the environment or from their direct application in products (Nawaz and Sengupta, 2019). The MPs are emerging water pollutants that have attracted considerable attention though with limited research on their fate in drinking water treatment plants (DWTPs) (Pivokonský et al., 2020). Investigations of some raw water samples from selected DWTPs have confirmed presence of MPs to levels greater than 4000 MPs per L (Pivokonsky et al., 2018; Mintenig et al., 2019). The MPS have also been detected in tap water (Mintenig et al., 2019; Shruti et al., 2020) as well as bottled drinking water (Mason et al., 2018; Oßmann et al., 2018; Schymanski et al., 2018). Inhalation of microplastics can pose a number of human health challenges such as genotoxicity inflammation, oxidative stress, apoptosis, necrosis, tissue damage, fibrosis and others as detailed by Wright and Kelly (2017). Currently, there is neither any standard limit for MP content in drinking water nor any treatment technology targeted directly for their removal (Wang et al., 2020d; Hou et al., 2021). Nevertheless, use of microfiltration (membrane bioreactors, micro-screen filtration, sand filtration) and AC filters have been proposed to remove microplastics to a certain extent (Fortin et al., 2019).

Microplastics have hydrophobic surfaces and can adsorb and concentrate many pollutants hence hampering pollutant removal efficiency during water treatment (Wright and Kelly, 2017; Zhang and Chen, 2020). The hydrophobicity, presence of surface charges, and surface functionalities of MPs could make them easily adsorbed by micro/mesoporous GAC. The MPs can be trapped into the porous structure of the AC hence enabling their removal from aqueous solution (Wang et al., 2020e). However, the removal mechanisms of MPs by GAC (either commercial or biomass based) are not clearly postulated and hence form a research gap.

### 8.2. Factors influencing adsorption of water contaminants by GAC

When using AC in aqueous phase, the adsorption process is a result of the interaction (electrostatic or non-electrostatic) between the carbon surface and the adsorbent (Mustafa and Asmatulu, 2020). When the adsorbent has the same electrostatic charge as the carbon surface, repulsion increases hence a decrease in adsorption capacity (Aygün et al., 2003). The choice of GAC should not only consider the affinity of the target compound but also GAC pore sizes (Piai et al., 2019). Adsorption can easily occur with compounds smaller or similar to the pore size of the AC (Mustafa and Asmatulu, 2020). The removal efficiency highly depends on the concentration of the contaminant, pH of the solution, contact time, adsorbent dosage, carbon surface functional groups, agitation speed, solution temperature among other factors. The influence of these factors on adsorption efficiency and capacity of GAC are briefly discussed below

#### 8.2.1. Solution pH

Solution pH affects adsorption efficiencies by influencing the degree of ionization of the contaminant (Baccar et al., 2010), and the state of chemically active sites of AC (Martín-Lara et al., 2019). The optimal pH is influenced by the point of zero charge ($pH_{PZC}$). The $pH_{PZC}$ is the pH at which the AC surface has a zero value. At $pH_{PZC}$, there is a charge boundary between negative and positive charge surface sites (Egirani et al., 2020). For instance, if the $pH_{PZC}$ is 8.5, solution pH < 8.5 will favor adsorption of anionic contaminants while solution pH > 8.5 will favor adsorption of cationic contaminants (Khadhri et al., 2019). An increase in the solution pH decreases the number of positively charged sites on AC which favors adsorption of cationic pollutants due to a reduction in electrostatic repulsions (Hejazifar et al., 2011; Dong et al., 2018). Conversely, this will decrease the adsorption of anionic pollutants (Baccar et al., 2010). The solution pH affects surface charges of the carbon (Foo and Hameed, 2013), and the electrostatic adsorbate-adsorbent interactions (Tran et al., 2019; Thakur et al., 2020). In cases where electrostatic attraction is not the main adsorption mechanism, solution pH may not greatly influence the adsorption efficiency (Nguyen et al., 2020).

#### 8.2.2. Activated carbon dose, and initial pollutant concentration

An increase in the adsorbent dosage increases the available surface area and sites for adsorption where by small quantities are susceptible to quicker saturation (Larous and Meniai, 2012). The decreased adsorption efficiency after an optimal dosage is attributed to a decline in number of binding sites while reduced adsorption capacity with increased dosage is attributed to an increased number of free binding sites on GAC surface (Abo El Naga et al., 2019). An increase in the contaminant concentration usually increases the adsorption capacity of GAC up to a certain extent though with decreased removal efficiency (Yossa et al., 2020). The increased adsorption capacity of AC at higher contaminant concentrations could be due to increased concentration gradient between the bulk solution and liquid-solid interface. A reduction in the adsorption efficiency at higher contaminant concentrations could be attributed to the saturation of the active adsorption sites on the surface of AC (Abo El Naga et al., 2019; Nagalakshmi et al., 2019).

#### 8.2.3. Contact time

The adsorption process involves the transfer of pollutant from the liquid phase into the solid AC. This implies that contact time between the two phases has an effect on mass transfer (Larous and Meniai, 2012). As the contact time is increased, the adsorption efficiency also increases until when any further increase in time will have no additional increase on adsorption denoting attainment of equilibrium. The equilibrium time is that time when the plot of adsorption efficiency against time appears asymptotic to the time axis (Nagalakshmi et al., 2019). On initiation of the adsorption process, there is a larger free surface area of AC and active adsorption sites which decrease with time (Çelebi, 2020). The optimal contact time depends on variables such GAC dosage, contaminant concentration, temperature, and AC surface groups.

#### 8.2.4. Activated carbon surface groups

The AC surfaces can be occupied by both acidic and basic functional groups. The acidic functional groups are generally categorized into lactones, phenols, carbonyls, and carboxyls exhibiting high cationic exchange capacities and oxygen content (Koutník et al., 2020). On the other hand, basic functional groups such as chromene and pyrone exhibit low oxygen content with high anionic exchange capacities (Crincoli et al., 2020). The adsorption mechanism of AC is greatly influenced by the type of functional groups available on its surface (Mallek et al., 2018). The carboxylic group is considered to be the most vital in interacting with most contaminants on the AC surface (Tran et al., 2019). The AC with acidic functional groups is best suited for adsorption of cationic contaminants such as heavy metals. The predominant functional group can be predicted from the $pH_{PZC}$ where by values greater than 7 indicate predominance of basic groups and values less than 7 indicating predominance of acidic groups. A higher $pH_{PZC}$ value (> 7) is also associated with a high surface hydrophobicity of the carbon material (Sajjadi et al., 2018). The presence and distribution of different functional groups on the AC surface are examined using the Fourier transform infrared (FT-IR) spectroscopy. The FT-IR spectra is a plot of absorbance (% transmittance) against wavelength ($cm^{-1}$). There are basically four regions of types of bonds that can be analyzed from the FT-IR spectra which include: single bonds detectable in higher wave number (4000–2500 $cm^{-1}$), triple bond (2500–2000 $cm^{-1}$), double bond (2000–1500 $cm^{-1}$) and the finger print region (1500–650 $cm^{-1}$) which is the characteristic of the molecule as a whole (Mohamed et al., 2017).

#### 8.2.5. Temperature

All adsorption processes are temperature dependent (Wang et al., 2020c). The adsorption process is said to be endothermic if an increase in temperature increases the adsorption capacity (Jung et al., 2016). Conversely, the process is exothermic and promoted by entropic contribution if the increase in temperature poorly influences adsorption (Villaescusa et al., 2011). An increase in the adsorption capacity at high temperatures could be attributed to the swelling effect within the internal structure of AC which opens the pores that allow mobility and adsorption of contaminants (Pathak and Mandavgane, 2015). The optimal condition for adsorption of different water contaminants using biomass based GAC are shown in Table 5.

### 8.3. Adsorption models

#### 8.3.1. Adsorption kinetics

Adsorption kinetics indicate the influence of contact time (adsorption rate) on the adsorption of a given contaminant of known concentration onto AC (Abo El Naga et al., 2019; Nagalakshmi et al., 2019). The kinetics measure diffusion of adsorbate into the pores, and are used in designing full scale contaminant removal systems (Sajjadi et al., 2019). They depend on concentration, temperature,

**Table 5**
Biomass waste based GAC used for removal of contaminants from water, optimal adsorption conditions and maximum adsorption capacities.

| Source-derived GAC | GAC adsorptive properties | | | | Water treatment application | | | | Reference |
|---|---|---|---|---|---|---|---|---|---|
| | Average particle size (mm) | Surface area ($S_{BET}$, $m^2/g$) | Pore volume ($cm^3/g$) | Pore diameter (nm) | Water contaminant | Optimal adsorption condition | Maximum adsorption capacity (mg/g) | Removal efficiency (%) | |
| *Haematoxylum campechianum* bark | 0.2–0.5 | 181.49 | 0.094 | 2.07 | 4-chlorophenol | $pH_{PZC}$ = 7.02; solution pH = 2; contaminant concentration = 100 mg/L; GAC dose = 10 g/L; temperature, 25 °C; contact time, 180 min | 92.58 | 89.2 | (Abatal et al., 2020) |
| Coconut shell | 3.25 | 1 022.4 | 0.492 | 1.516 | Chromium (VI) ions | Solution pH = 3.5, contaminant concentration = 1000 mg/L, GAC dose = 10 g/L; temperature, 30 °C; contact time, 50 h | 45.2 | 48 | (Wang et al., 2020c) |
| *Haematoxylum campechianum* bark | 0.2–0.5 | 181.49 | 0.094 | 2.07 | 4-nitrophenol | $pH_{PZC}$ = 7.02; solution pH = 2; contaminant concentration = 100 mg/L; GAC dose = 10 g/L; temperature, 25 °C; contact time,180 min | 84.80 | 93.2 | (Abatal et al., 2020) |
| Sugarcane bagasse | 0.5 | 1 145 | 1.3 | 4.54 | Sodium diclofenac | $pH_{PZC}$ = 7.3 solution pH = 2, contaminant concentration = 50 mg/L, GAC dose = 0.4 g/L; contact time, 15 min | 315.00 | 95.6 | (Abo El Naga et al., 2019) |
| Avocado kernel seeds | 0.67 | 299.9 | 0.172 | 1.34 | Flouride | $pH_{PZC}$ = 7.20; solution pH = 7, contaminant concentration = 50 mg/L; GAC dose = 2 g/L; contact time, 24 h; temperature, 30 °C | 19.99 | 89.3 | (Salomón-Negrete et al., 2018) |
| Pistachio wood | 0.5–2.0 | 1 445 | 0.901 | 2.49 | Mercury | $pH_{PZC}$ = 9.6; solution pH = 7, contaminant concentration = 25 mg/L; GAC dose = 2 g/L; contact time, 20 min; temperature, 25 °C | 190.2 | 97.9 | (Sajjadi et al., 2018) |
| Pistachio wood | 0.5–2.0 | 1 884 | 0.994 | 2.11 | Lead (II) ions | $pH_{PZC}$ = 8.1; solution pH = 6, contaminant concentration = 25 mg/L; GAC dose = 0.2 g/L; contact time, 2 h; temperature, 25 °C | 190.2 | 93.7 | (Sajjadi et al., 2019) |
| Date press cake | 0.5–1.0 | 2 025.9 | 0.932 | 1.839 | Chromium (VI) ions | $pH_{PZC}$ = 7.0; solution pH = 2; contaminant concentration = 300 mg/L; GAC dose = 1 g/L; contact time, 180 min | 282.8 | 94.6 | (Norouzi et al., 2018) |
| Phoenix tree leaves | 5–6 | 166.3 | 0.276 | 1.077 | Lead (II) ions | Solution pH = 6, contaminant concentration = 100 mg/L; GAC dose = 5 g/L; contact time, 24 h; temperature, 25 °C | 71 | 99.2 | (Liang et al., 2016) |
| Coffee ground | 2.03 | 704.23 | 0.293 | 2.20 | Acid orange 7 | $pH_{PZC}$ = 7.6; solution pH = 3, contaminant concentration = 200 mg/L; GAC dose = 2 g/L; contact time, 24 h; temperature, 30 °C | 665.9 | 97.4 | (Jung et al., 2016) |
| Grape fruit peels | 0.25–0.35 | – | – | – | Copper (II) ions | $pH_{PZC}$ = 6.8; solution pH = 6.3, contaminant concentration = 60 mg/L; GAC dose = 0.5 g/L; contact time, 210 min; temperature, 318 K | 48.22 | 88.2 | (Semercïöz et al., 2017) |
| Baobab seed hulls | 0.8–1.6 | 1 086 | 2.3 | – | Diuron | Solution pH = 8.5, temperature, 32 °C; GAC dose = 0.1 g/L, contaminant concentration = 13 mg/L | – | 51 | (Ndjientcheu et al., 2020) |

(*continued on next page*)

**Table 5** (*continued*)

| Source-derived GAC | GAC adsorptive properties | | | | Water treatment application | | | | Reference |
|---|---|---|---|---|---|---|---|---|---|
| | Average particle size (mm) | Surface area ($S_{BET}$, $m^2/g$) | Pore volume ($cm^3/g$) | Pore diameter (nm) | Water contaminant | Optimal adsorption condition | Maximum adsorption capacity (mg/g) | Removal efficiency (%) | |
| Prawn carapace | 0.425–0.6 | 56.3 | 0.17 | – | Cerium (III) ions | Solution pH = 6, contaminant concentration = 300 mg/L; GAC dose = 0.25 g/L; contact time, 6 h; temperature, 40 °C | 218.3 | – | (Varsihini et al., 2014) |
| Corn style | 0.425–0.6 | 47.3 | 0.12 | – | Cerium (III) ions | Solution pH = 6, contaminant concentration = 250 mg/L; GAC dose = 0.25 g/L; contact time, 6 h; temperature, 40 °C | 180.2 | – | (Varsihini et al., 2014) |
| Corn cob | 0.6–0.8 | – | – | – | Flouride | $pH_{PZC}$ = 2.3; solution pH = 6, contaminant concentration = 13 mg/L; GAC dose = 2 g/L; contact time, 5 h; | 5.8 | 89 | (Gebrewold et al., 2019) |
| Rice husks | 0.6–0.8 | – | – | – | Flouride | $pH_{PZC}$ = 6.7; solution pH = 4, contaminant concentration = 18 mg/L; GAC dose = 2 g/L; contact time, 3 h; | 7.9 | 91 | (Gebrewold et al., 2019) |
| *Parkinsonia aculeata* wood Sawdust | 0.375 | 768 | 0.37 | 3.8 | Nitrate ions | $pH_{PZC}$ = 6.8; solution pH= 2; contaminant concentration = 1.61 mmol/L, GAC dose = 100 g/L; temperature, 25 °C | 0.30 mmol/g | 68 | Nunell et al., 2012) |
| Pumpkin seed hulls | 0.5–1.0 | 737.90 | 0.37 | 2.261S | 2, 4-D | $pH_{PZC}$ = 6; solution pH = 2, contaminant concentration = 50 mg/L, GAC dose = 1 g/L; temperature, 30 °C; contact time, 10 h | 260.79 | 98.28 | (Njoku et al., 2013) |
| Palm oil fronds | 2 | 1 237.13 | 0.667 | 2.16 | Bentazon | Contaminant concentration = 100 mg/L, GAC dose = 3 g/L; temperature, 30 °C; | – | 95 | (Salman, 2014) |
| Palm oil fronds | 2 | 1 237.13 | 0.667 | 2.16 | Carbofuran | Contaminant concentration = 100 mg/L, GAC dose = 3 g/L; temperature, 30 °C; | – | 93 | (Salman, 2014) |
| Palm oil fronds | 2 | 1237.13 | 0.667 | 2.16 | 2, 4-D | Contaminant concentration = 100 mg/L, GAC dose = 3 g/L; temperature, 30 °C; | – | 95 | (Salman, 2014) |
| *Argania spinasa* tree nutshells | 1–2 | 1 159 | 0.64 | – | Diclofenac | Contaminant concentration = 50 mg/L, GAC dose = 0.1 g/L; temperature, 25 °C; | 121.9 | – | (El Mouchtari et al., 2020) |
| *Argania spinasa* tree nutshells | 1–2 | 1 159 | 0.64 | – | Carbamazepine | Contaminant concentration = 50 mg/L, GAC dose = 0.1 g/L; temperature, 25 °C; | 175.4 | – | (El Mouchtari et al., 2020) |
| Langsat empty fruit bunch | 0.50–0.71 | 1 070.36 | 0.83 | 3.671 | 2, 4-D | Solution pH =2, contaminant concentration = 200 mg/L, GAC dose = 1 g/L; temperature, 30 °C; contact time, 24 h | 261.2 | 93.11 | (Njoku et al., 2015) |
| Date stones | 1–2 | 852 | 0.671 | 3.15 | Levofloxacin | Solution pH = 7; contaminant concentration = 50 mg/L; GAC dose = 0.15 g/L; contact time, 90 min | – | 97.01 | (Darweesh and Ahmed, 2017) |

adsorbent properties (surface chemistry, surface areas, pore size), and interaction energy between adsorbent and adsorbate (Ouyang et al., 2020). Different kinetic models such as pseudo-first order, pseudo second order, Elovich, and intraparticle diffusion model have been used to predict the rate of reaction for a sorption system in aqueous solution. Among these, the pseudo-first order (Eq. (1)) and pseudo second order (Eq. (2)) models (Kutluay et al., 2019) have been proven to be the most effective for the adsorption phenomena (Ganguly et al., 2020). Pseudo-first order model assumes that the adsorption process is dependent on the number of available binding sites for equilibrium established at contact time below 30 min (Beltrame et al., 2018). Pseudo-second order model assumes that contaminants are adsorbed by both internal and external mass transfer mechanisms (Lütke et al., 2019).

$$q_t = q_e\left(1 - e^{-k_1 t}\right) \tag{1}$$

$$q_t = \frac{{q_e}^2 k_2 t}{1 + q_e k_2 t} \tag{2}$$

where $q_e$ and $q_t$ are the amounts of contaminant (mg/g) adsorbed on adsorbent at equilibrium and at time $t$ (min) respectively, $k_1$ ($min^{-1}$), and $k_2$ (g/(mg•min)) are pseudo first order and pseudo second order rate constants, respectively. Parameters $q_e$ and $q_t$ are calculated from Eqs. (3) and (4), respectively as described by Eeshwarasinghe et al. (2019).

$$q_e = \frac{\left(C_o - C_e\right) \cdot V}{M} \tag{3}$$

$$q_t = \frac{\left(C_o - C_t\right) \cdot V}{M} \tag{4}$$

where $C_o$ is initial concentration of contaminant (mg/L), $C_e$ is equilibrium concentration of contaminant (mg/L), $C_t$ is concentration of contaminant at time $t$ (mg/L), $V$ is volume of the solution (L), and $M$ is mass of the adsorbent (g). The adsorption of the contaminant by the adsorbent can be evaluated using the fitness of the kinetic models (Nagalakshmi et al., 2019). This fitness is assessed using the squared sum of errors (SSE) values (Eq. (5)) with the best model for the system being that with the lowest SSE values. The best model usually has the highest correlation coefficient ($R^2$) and $q_{e(cal)}$ (Abo El Naga et al., 2019).

$$\mathrm{SSE} = \sum \frac{\left(q_{e(expt)} - q_{e(cal)}\right)^2}{{q_{e(expt)}}^2} \tag{5}$$

where, $q_{e(expt)}$ and $q_{e(cal)}$ are experimental, and kinetic model sorption capacities (mg/g) of the contaminants, respectively.

### 8.3.2. Adsorption isotherms

Adsorption isotherms reveal the distribution of adsorbate molecules between the liquid phase and the solid phase when the adsorption process reaches equilibrium (Araga et al., 2017; Beltrame et al., 2018). In other words, they are plots of equilibrium relationship between the amount of contaminant left in solution and the amount of contaminant that is on the surface of the adsorbent (Menya et al., 2018). The four commonly used isotherms for liquid/solid systems are the Dubinin-Radushkevich, Temkin, Langmuir, and Freundlich. The Langmuir, and Freundlich isotherms are the commonly used in water treatment (Menya et al., 2018). Langmuir model (Eq. (6)) assumes monolayer sorption onto a completely homogenous surface with a finite number of identical sites, and with no interaction between adsorbed molecules (Li et al., 2014). On the other hand, Freundlich model (Eq. (7)) assumes multilayer adsorption and surface heterogeneity of the adsorbent (Fu et al., 2017b). The suitable isotherm for the sorption of the contaminant onto GAC is that with a smaller SSE value and higher coefficient of determination ($R^2$) value (Nagalakshmi et al., 2019)

$$\frac{C_e}{q_e} = \frac{1}{Q_m K_L} + \frac{1}{Q_m} C_e \tag{6}$$

$$q_e = K_F {C_e}^{\frac{1}{n}} \tag{7}$$

where, $Q_m$ is the maximum adsorption capacity (mg/g), $K_L$ is the Langmuir adsorption constant (L/mg), $K_F$ and n are Freundlich constants. The $K_L$ reflects the apparent adsorption energy (Fu et al., 2017b), and $K_F$ is related to the adsorption capacity (Nikić et al., 2019), while n is the adsorptive intensity relating the adsorption driving force and the distribution of the energy sites on the adsorbent (Menya et al., 2018). The values of the kinetic and isotherm models for adsorption studies of biomass based GAC are shown in Table 6.

### 8.4. Adsorption mechanism

The adsorption capacity and mechanism of the contaminant depend on the adsorbent properties (Tran et al., 2019). The active sites of the porous carbon improve the mass transfer of the pollutants to the internal pores where they interact with the hydroxyl and other free radicals thus enabling the adsorption process (Hao et al., 2021). The adsorption of contaminants onto the surface of AC is due to surface energy which is a combination of a number of interactions (Ouyang et al., 2020). The adsorption energy is established

**Table 6**
Pseudo-first order, Pseudo-second order, Langmuir and Freundlich adsorption model coefficients for different waste based GAC for removal of contaminants from water.

| Source of waste based GAC | Contaminant | Pseudo-first order model | | Pseudo-second order model | | Langmuir model | | | Freundlich model | | | Reference |
|---|---|---|---|---|---|---|---|---|---|---|---|---|
| | | $q_{e(expt)}$ (mg/g) | $R^2$ | $q_{e(expt)}$ (mg/g) | $R^2$ | $K_L$ (L/mg) | $Q_m$ (mg/g) | $R^2$ | $K_F$ (mg/g)(L/mg)$^{1/n}$ | 1/n | $R^2$ | |
| *Limonia acidissima* shell | Iron ions | 48.13 | 0.861 | 48.13 | 0.999 | 0.610 | 50.38 | 0.970 | 53.400 | 0.625 | 0.918 | (Das and Mishra, 2020) |
| *Tithonia diversifolia* | Bisphenol A | 9.625 | 0.895 | 9.625 | 0.999 | 0.007 | 15.69 | 0.997 | 1.19 | 0.319 | 0.764 | (Supong et al., 2019) |
| Elaeagnus angustifolia seeds | Benzene | 49.95 | 0.840 | 55.91 | 1.000 | 0.068 | 99.85 | 0.999 | 11.586 | 0.521 | 0.789 | (Kutluay et al., 2019) |
| Black wattle bark | Phenol | 63.69 | 0.985 | 75.07 | 0.998 | 0.037 | 98.57 | 0.932 | 20.140 | 3.710 | 0.998 | (Lütke et al., 2019) |
| Pistachio wood waste | Lead ions | 165.70 | 0.994 | 178.40 | 1.000 | 1.983 | 190.20 | 0.999 | 113.700 | 0.268 | 0.912 | (Sajjadi et al., 2019) |
| Peanut shells | Acid yellow 36 | 26.70 | 0.961 | 52.60 | 0.999 | 0.940 | 66.70 | 0.988 | 32.500 | 0.387 | 0.954 | (Garg et al., 2019) |
| Pineapple leaves | Caffeine | 141.70 | 0.924 | 149.50 | 0.998 | 0.088 | 155.50 | 0.987 | 44.370 | 0.224 | 0.885 | (Beltrame et al., 2018) |
| Tomato stem | Congo red | – | – | – | – | 0.087 | 158.73 | 0.999 | 72.277 | 0.139 | 0.956 | (Fu et al., 2017b) |
| Waste tea | Oxytetracycline | 205.61 | 0.979 | 294.68 | 0.989 | 0.151 | 273.70 | 0.747 | 119.260 | 0.161 | 0.959 | (Kan et al., 2017) |

using Eq. (8):

$$E_{\text{adsorp}} = E_{\text{pol, GAC}} - \left(E_{\text{pol}} + E_{\text{GAC}}\right) \quad (8)$$

where $E_{\text{adsorp}}$ is the adsorption energy, $E_{\text{pol,GAC}}$ is the total energy of pollutant and activated carbon in equilibrium state, $E_{\text{pol}}$ is the total energy of the pollutant molecule, and $E_{\text{GAC}}$ is total energy of granular activated carbon. Adsorption energy less than −30 kJ/mol, indicates a physisorption interaction while that higher than −50 kJ/mol indicates a chemisorption interaction (Khadhri et al., 2019).

Physical adsorption implies that only weak interaction forces such ionic, electrostatic, hydrogen bonding, and dipole interactions are involved between the adsorbent and adsorbate (Bojić et al., 2017; Khadhri et al., 2019). The adsorptive process is seldom purely physical or chemical though sometimes physiochemical mechanisms are involved (Alharbi et al., 2020; Ighalo et al., 2021). Such mechanisms involve formation of positively charged sites, $\pi$-$\pi$ dispersion, donor-acceptor electrostatic interaction, repulsive electrostatic interaction, formation of strong inner-sphere surface complexes, formation of hydrogen bonds with neighboring solutes or adsorbent oxygen group, van der Waal's forces and dipole-dipole forces.

Electrostatic interaction constitutes of electric forces of attraction and repulsion between adsorbate and adsorbent (Ouyang et al., 2020). If electrostatic attraction plays a primary role in adsorption, then changes in solution pH significantly affects the adsorption capacity otherwise it ceases to contribute to adsorption (Tran et al., 2017; Salomón-Negrete et al., 2018). Hydrogen bonds are formed in presence of hydrogen donor/acceptor chemical groups on both the contaminant and AC (Ouyang et al., 2020). The contribution of hydrogen bonding in adsorption can be identified from the FTIR spectra on the AC surface before and after adsorption. A decrease in the –OH peak intensity, and its shift towards higher wave numbers after adsorption indicates the presence of hydrogen bonding (Tran et al., 2017).

Pore filling occurs when there is an interaction between the contaminants already adsorbed on the surface of AC and those that are free in the solution (Li et al., 2020b). If an increase in surface area of AC does not guarantee an increased adsorption capacity, then pore filling is likely not to be contributing to the adsorption mechanism (Sajjadi et al., 2018). A remarkable decrease in the surface area and total pore volume of AC after adsorption could indicate that pore filling was the dominant adsorption mechanism (Tran et al., 2017; Nguyen et al., 2020). The $\pi$-$\pi$ interaction is described as the dispersive interaction through the delocalized $\pi$ electrons of oxygen-free Lewis basic sites of AC, and the free electrons of the contaminant in the aromatic rings (Chiang et al., 2020). The contribution of $\pi$- $\pi$ interaction in adsorption is evident when there is a decreased intensity in the aromatic C = C bonds on the surface of AC and their increase in wavenumber after adsorption (Tran et al., 2017). Besides the FT-IR, other advanced spectroscopy such as the scanning electron microscopy, field emission transmission electron microscopy, Ultraviolet-visible spectroscopy, Raman spectroscopy, X-ray diffraction analysis, X-ray photoelectron spectroscopy can also indicate the different adsorption mechanisms as discussed in different studies (Benabid et al., 2019; Hou et al., 2020).

The adsorption mechanism can also be predicted by various computational simulation approaches such as Grand canonical Monte Carlo (GCMC), molecular dynamics (MD), Hartree- Fock (HeF) calculations, and drift functional theory (DFT) (Hamed Mashhadzadeh et al., 2018; An et al., 2019; Kuntail et al., 2019). These simulations provide insights on the adsorption mechanism at a microscopic level (Benabid et al., 2019) thus offering sufficient description of the kinetics and thermodynamics of the adsorption process (Hu et al., 2020). Amongst these approaches, DFT is considered as a good estimation of the adsorption mechanism (Hamed Mashhadzadeh et al., 2018) because it accounts for more details about electron-electron, electron-ion and ion-ion interactions, which are disregarded in other computational methods (Ganji et al., 2012). The DFT calculations can also indicate the adsorption energy, geometry orientation, vibration frequencies, equilibrium distance between the pollutant and the carboneous surface, as well as the length of different bonds on the AC surfaces before, and after adsorption. In addition, the DFT studies also indicate how the presence and interaction of different functional groups on the AC surface influences the adsorption process (Supong et al., 2019; Liu et al., 2020b).

For a theoretical study involving the interaction of AC with an adsorbate, the most important requirement is to first establish a correct model for the AC surface (Supong et al., 2019). The AC can take on different models such as the zigzag and arm chair, with a number of active sites for adsorption purposes. It is of great importance to establish a reasonable model in order to investigate the interactions of the pollutant with AC surfaces (Shen et al., 2018). The most stable model is one with the highest negative adsorption energy and it usually exhibits the greatest adsorption tendency of a pollutant under study (Shen et al., 2018; Xie et al., 2021).

### 8.5. Regeneration of waste based GAC

The maximum adsorption capacity occurs at the initial stages due to availability of a greater surface area that provides free binding sites for the sorption of adsorbent (Thakur et al., 2020). At certain level of use, the carbon reaches a saturation point and losses its adsorption efficiency. This is due to presence of oxygen-acid surface groups on the carbon (Hossain et al., 2020) that are induced by the adsorbate hence reducing the adsorption capacity of the adsorbent (Talat et al., 2018). One of the key advantages of GAC over PAC is the ability to be regenerated after reaching a saturation point. The regeneration of AC is essential in reducing: 1) the accumulation of solids from the used adsorbent (Santoso et al., 2020), 2) fouling effect of the carbon surface (Wang et al., 2020a), and 3) the operational costs (Hossain et al., 2020). Contaminant removal and regeneration efficiencies decrease with increased numbers of adsorption-regeneration cycles (Fu et al., 2017b). The common regeneration techniques are thermal volatilization, wet oxidation, chemical, electrochemical, bio-regeneration, and solvent regeneration (El Gamal et al., 2018). The most predominant is the thermal regeneration (800–1000 °C) in presence of steam or $CO_2$ (Ao et al., 2018). However, the successive heating and cooling associated with thermal regeneration negatively affect the structural properties of AC leading to significant reduction in surface area (Da and Awad, 2017).

## 9. Future prospects

The reviewed data indicate that granular activated carbon can be generated from waste bio materials, and this carbon can effectively remove a number of contaminants from water. For high density wastes such as shells and seeds, granules can easily be generated by reduction of the waste to the desired granular size followed by carbonization and then activation. For low density and light waste materials, a granulation step is needed to produce strong granules that will not disintegrate in water. These granules can be produced directly from the raw precursor, carbonized precursor or from powdered activated carbon with or without use of binders. However, the effects of these preparation routes on the quality of derived GAC and its adsorption capacity are not known and therefore form a research gap. The selection of optimal activation methods and granulation factors such as pressure, temperature, and time need to be investigated for each preparation pathway. The economic and technical feasibilities of preparing waste based GAC employing different pathways are also yet to be investigated. There is also a need to evaluate the abrasion resistance of GAC prepared using different paths so as to ascertain their use under high pressure fluid flows. Optimization of process parameters from different preparation pathways using response surface methodology by design expert as well as life cycle assessment and material flow analysis studies needs to be investigated. The effect of binder type (organic or inorganic) and characteristics of the binders on the properties of the derived carbons is also not well established. There is also a dearth of scientific information on the adsorption studies of biomass based GAC for removal of microplastics in aqueous solutions. Lastly, most adsorption studies have been conducted in batch experiments. However, continuous fixed bed adsorption experiments using real water sources are more viable in assessing drinking water treatment processes, and require regeneration of the carbons for environmental and economic considerations. Therefore, more studies on the practical use of waste based GAC in continuous columns, and their regeneration potential need to be conducted.

## 10. Conclusions

The vast applications of GACs especially in aqueous solutions have increased its demand in many industrial applications. This has increased a search for alternative sources of these carbons to replace commercial GAC that is otherwise expensive and obtained from non-renewable sources. In this review, production of GAC from waste materials has been presented. Production steps such as granulation with and without binders as well as different carbonization and activation methods used to enhance strength and increase attrition resistance of the waste based GAC have been presented. The use of these GACs for water treatment has exhibited a great potential sometimes performing better than the commercial carbons depending on the target contaminant. Much as the optimal conditions for preparation of these carbons has been extensively studied, and there is a dearth of studies on how different preparation pathways affect the use of these carbons in continuous bed columns as well as regeneration potentials. Due to a variation in the composition of waste biomaterials depending on many factors such as origin and agronomic practices, there is a need for more detailed studies on production, optimization, and applications of waste based granular activated carbon.

## Declaration of Competing Interest

The authors declare that they have no known competing financial interests or personal relationships that could have appeared to influence the work reported in this paper.

## Acknowledgment

This research was made possible with support from the Government of the Republic of Uganda through Makerere University Research and Innovations Fund (RIF1/CEDAT/015).

## References

Abatal, M., Anastopoulos, I., Giannakoudakis, D.A., Olguin, M.T., 2020. Carbonaceous material obtained from bark biomass as adsorbent of phenolic compounds from aqueous solutions. J. Environ. Chem. Eng. 8, 103784.
Abo El Naga, A.O., El Saied, M., Shaban, S.A., El Kady, F.Y., 2019. Fast removal of diclofenac sodium from aqueous solution using sugar cane bagasse-derived activated carbon. J. Mol. Liq. 285, 9–19.
Acevedo-Páez, J.C., Durán, J.M., Posso, F., Arenas, E., 2020. Hydrogen production from palm kernel shell: kinetic modeling and simulation. Int. J. Hydrog. Energy 45, 25689–25697.
Aguayo-Villarreal, I.A., Bonilla-Petriciolet, A., Muñiz-Valencia, R., 2017. Preparation of activated carbons from pecan nutshell and their application in the antagonistic adsorption of heavy metal ions. J. Mol. Liq. 230, 686–695.
Ahmad, F., Daud, W.M.A.W., Ahmad, M.A., Radzi, R., Azmi, A.A., 2013. The effects of $CO_2$ activation, on porosity and surface functional groups of cocoa (*Theobroma cacao*)-Shell based activated carbon. J. Environ. Chem. Eng. 1, 378–388.
Ahmed, M.B., Zhou, J.L., Ngo, H.H., Guo, W.S., Thomaidis, N.S., Xu, J., 2017. Progress in the biological and chemical treatment technologies for emerging contaminant removal from wastewater: a critical review. J. Hazard. Mater. 323, 274–298.
Ahmed, M.J., Theydan, S.K., 2012. Physical and chemical characteristics of activated carbon prepared by pyrolysis of chemically treated date stones and its ability to adsorb organics. Powder Technol 229, 237–245.
Alharbi, N.S., Hu, B.W., Hayat, T., Rabah, S.O., Alsaedi, A., Zhuang, L., Wang, X.K., 2020. Efficient elimination of environmental pollutants through sorption-reduction and photocatalytic degradation using nanomaterials. Front. Chem. Sci. Eng. 14, 1124–1135.
Ali, P.A., Reza, M.M., Hossein, S.M., 2010. Removal of dissolved organic carbon by multi-walled carbon nanotubes, powdered activated carbon and granular activated carbon. Res. J. Chem. Environ. 14, 59–66.
Alslaibi, T.M., Abustan, I., Ahmad, M.A., Foul, A.A., 2013. A review: production of activated carbon from agricultural byproducts via conventional and microwave heating. J. Chem. Technol. Biotechnol. 88, 1183–1190.
Alves, A.A.D.A., Ruiz, G.L.D.O., Nonato, T.C.M., Müller, L.C., Sens, M.L., 2019. Performance of the fixed-bed of granular activated carbon for the removal of pesticides from water supply. Environ. Technol. 40, 1977–1987.

Alves, J.L.F., da Silva, J.C.G., Mumbach, G.D., Domenico, M.D., da Silva Filho, V.F., de Sena, R.F., Machado, R.A.F., Marangoni, C., 2020. Insights into the bioenergy potential of jackfruit wastes considering their physicochemical properties, bioenergy indicators, combustion behaviors, and emission characteristics. Renew. Energy 155, 1328–1338.
Amarasekara, A., Tanzim, F.S., Asmatulu, E., 2017. Briquetting and carbonization of naturally grown algae biomass for low-cost fuel and activated carbon production. Fuel 208, 612–617.
An, Y., Fu, Q., Zhang, D., Wang, Y., Tang, Z., 2019. Performance evaluation of activated carbon with different pore sizes and functional groups for VOC adsorption by molecular simulation. Chemosphere 227, 9–16.
An, Y., Tahmasebi, A., Zhao, X.H., Matamba, T., Yu, J.L., 2020. Catalytic reforming of palm kernel shell microwave pyrolysis vapors over iron-loaded activated carbon: enhanced production of phenol and hydrogen. Bioresour. Technol. 306, 123111.
Ao, W.Y., Fu, J., Mao, X., Kang, Q.H., Ran, C.M., Liu, Y., Zhang, H.D., Gao, Z.P., Li, J., Liu, G.Q., Dai, J.J., 2018. Microwave assisted preparation of activated carbon from biomass: a review. Renew. Sustain. Energy Rev. 92, 958–979.
Araga, R., Soni, S., Sharma, C.S., 2017. Fluoride adsorption from aqueous solution using activated carbon obtained from KOH-treated jamun (*Syzygium cumini*) seed. J. Environ. Chem. Eng. 5, 5608–5616.
Arami-Niya, A., Wan Daud, W.M.A., Mjalli, F.S., Abnisa, F., Shafeeyan, M.S., 2012. Production of microporous palm shell based activated carbon for methane adsorption: modeling and optimization using response surface methodology. Chem. Eng. Res. Des. 90, 776–784.
Aransiola, E.F., Oyewusi, T.F., Osunbitan, J.A., Ogunjimi, L.A.O., 2019. Effect of binder type, binder concentration and compacting pressure on some physical properties of carbonized corncob briquette. Energy Rep. 5, 909–918.
Aworn, A., Thiravetyan, P., Nakbanpote, W., 2008. Preparation and characteristics of agricultural waste activated carbon by physical activation having micro- and mesopores. J. Anal. Appl. Pyrolysis 82, 279–285.
Aygün, A., Yenisoy-Karakaş, S., Duman, I., 2003. Production of granular activated carbon from fruit stones and nutshells and evaluation of their physical, chemical and adsorption properties. Microporous Mesoporous Mater. 66, 189–195.
Baccar, R., Blánquez, P., Bouzid, J., Feki, M., Sarrà, M., 2010. Equilibrium, thermodynamic and kinetic studies on adsorption of commercial dye by activated carbon derived from olive-waste cakes. Chem. Eng. J. 165, 457–464.
Bae, W., Kim, J., Chung, J., 2014. Production of granular activated carbon from food-processing wastes (walnut shells and jujube seeds) and its adsorptive properties. J. Air Waste Manag. Assoc. 64, 879–886.
Bandara, Y.W., Gamage, P., Gunarathne, D.S., 2020. Hot water washing of rice husk for ash removal: the effect of washing temperature, washing time and particle size. Renew. Energy 153, 646–652.
Başakçılardan Kabakcı, S., Baran, S.S., 2019. Hydrothermal carbonization of various lignocellulosics: fuel characteristics of hydrochars and surface characteristics of activated hydrochars. Waste Manag. 100, 259–268.
Beltrame, K.K., Cazetta, A.L., de Souza, P.S.C., Spessato, L., Silva, T.L., Almeida, V.C., 2018. Adsorption of caffeine on mesoporous activated carbon fibers prepared from pineapple plant leaves. Ecotoxicol. Environ. Saf. 147, 64–71.
Benabid, S., Streit, A.F.M., Benguerba, Y., Dotto, G.L., Erto, A., Ernst, B., 2019. Molecular modeling of anionic and cationic dyes adsorption on sludge derived activated carbon. J. Mol. Liq. 289, 111119.
Benstoem, F., Becker, G., Firk, J., Kaless, M., Wuest, D., Pinnekamp, J., Kruse, A., 2018. Elimination of micropollutants by activated carbon produced from fibers taken from wastewater screenings using hydrothermal carbonization. J. Environ. Manag. 211, 278–286.
Bergna, D., Hu, T., Prokkola, H., Romar, H., Lassi, U., 2020. Effect of some process parameters on the main properties of activated carbon produced from peat in a lab-scale process. Waste Biomass Valorization 11, 2837–2848.
Bhatnagar, A., Kaczala, F., Hogland, W., Marques, M., Paraskeva, C.A., Papadakis, V.G., Sillanpää, M., 2014. Valorization of solid waste products from olive oil industry as potential adsorbents for water pollution control: a review. Environ. Sci. Pollut. Res. Int. 21, 268–298.
Bhatnagar, A., Sillanpää, M., 2017. Removal of natural organic matter (NOM) and its constituents from water by adsorption: a review. Chemosphere 166, 497–510.
Bhatnagar, A., Tolvanen, H., Konttinen, J., 2020. Potential of stepwise pyrolysis for on-site treatment of agro-residues and enrichment of value-added chemicals. Waste Manag. 118, 667–676.
Bhomick, P.C., Supong, A., Karmaker, R., Baruah, M., Pongener, C., Sinha, D., 2019. Activated carbon synthesized from biomass material using single-step KOH activation for adsorption of fluoride: experimental and theoretical investigation. Korean J. Chem. Eng. 36, 551–562.
Bojić, D., Momčilović, M., Milenković, D., Mitrović, J., Banković, P., Velinov, N., Nikolić, G., 2017. Characterization of a low cost *Lagenaria vulgaris* based carbon for ranitidine removal from aqueous solutions. Arab. J. Chem. 10, 956–964.
Brunner, A.M., Bertelkamp, C., Dingemans, M.M.L., Kolkman, A., Wols, B., Harmsen, D., Siegers, W., Martijn, B.J., Oorthuizen, W.A., Laak, ter, 2020. Integration of target analyses, non-target screening and effect-based monitoring to assess OMP related water quality changes in drinking water treatment. Sci. Total Environ. 705, 135779.
Bu, Q., Lei, H.W., Wang, L., Wei, Y., Zhu, L., Liu, Y.P., Liang, J., Tang, J.M., 2013. Renewable phenols production by catalytic microwave pyrolysis of Douglas fir sawdust pellets with activated carbon catalysts. Bioresour. Technol. 142, 546–552.
Cagnon, B., Py, X., Guillot, A., Stoeckli, F., Chambat, G., 2009. Contributions of hemicellulose, cellulose and lignin to the mass and the porous properties of chars and steam activated carbons from various lignocellulosic precursors. Bioresour. Technol. 100, 292–298.
Cai, Z.H., Deng, X.C., Wang, Q., Lai, J.J., Xie, H.L., Chen, Y.D., Huang, B., Lin, G.F., 2020. Core-shell granular activated carbon and its adsorption of trypan blue. J. Clean. Prod. 242, 118496.
Cai, Z.H., Yang, X., Lin, G.F., Chen, C.X., Chen, Y.D., Huang, B., 2018. On preparing highly abrasion resistant binderless and in situ N-doped granular activated carbon. RSC Adv 8, 20327–20333.
Cao, Q., Xie, K.C., Lv, Y.K., Bao, W.R., 2006. Process effects on activated carbon with large specific surface area from corn cob. Bioresour. Technol. 97, 110–115.
Cao, Y.Y., Xiao, W.H., Shen, G.H., Ji, G.Y., Zhang, Y., Gao, C.F., Han, L.J., 2019. Carbonization and ball milling on the enhancement of Pb(II) adsorption by wheat straw: competitive effects of ion exchange and precipitation. Bioresour. Technol. 273, 70–76.
Çelebi, H., 2020. Recovery of detox tea wastes: usage as a lignocellulosic adsorbent in $Cr^{6+}$ adsorption. J. Environ. Chem. Eng. 8, 104310.
Chang, G.Z., Shi, P.C., Guo, Y.N., Wang, L.Y., Wang, C.P., Guo, Q.J., 2020. Enhanced pyrolysis of palm kernel shell wastes to bio-based chemicals and syngas using red mud as an additive. J. Clean. Prod. 272, 122847.
Chavoshani, A., Hashemi, M., Mehdi Amin, M., Ameta, S.C., 2020. Risks and Challenges of Pesticides in Aquatic environments. Micropollutants and Challenges. Elsevier, Amsterdam, pp. 179–213.
Cheng, C., Liu, H., Dai, P., Shen, X.X., Zhang, J., Zhao, T.Y., Zhu, Z.R., 2016. Microwave-assisted preparation and characterization of mesoporous activated carbon from mushroom roots by phytic acid ($C_6H_{18}O_{24}P_6$) activation. J. Taiwan Inst. Chem. Eng. 67, 532–537.
Chiang, C.H., Chen, J., Lin, J.H., 2020. Preparation of pore-size tunable activated carbon derived from waste coffee grounds for high adsorption capacities of organic dyes. J. Environ. Chem. Eng. 8, 103929.
Chili, C.A., Westerhoff, P., Ghosh, A., 2012. GAC removal of organic nitrogen and other DBP precursors. J. Am. Water Work. Assoc. 104, E406–E415.
Chou, C.S., Lin, S.H., Lu, W.C., 2009. Preparation and characterization of solid biomass fuel made from rice straw and rice bran. Fuel Process. Technol. 90, 980–987.
Chowdhury, Z.Z., Abd Hamid, S.B., Das, R., Hasan, M.R., Zain, S.M., Khalid, K., Uddin, M.N., 2013. Preparation of carbonaceous adsorbents from lignocellulosic biomass and their use in removal of contaminants from aqueous solution. Bioresources 8, 6523–6555.
Colantoni, A., Evic, N., Lord, R., Retschitzegger, S., Proto, A.R., Gallucci, F., Monarca, D., 2016. Characterization of biochars produced from pyrolysis of pelletized agricultural residues. Renew. Sustain. Energy Rev. 64, 187–194.
Crincoli, K.R., Jones, P.K., Huling, S.G., 2020. Fenton-driven oxidation of contaminant-spent granular activated carbon (GAC): GAC selection and implications. Sci. Total. Environ. 734, 139435.
Da, E., Awad, A., 2017. Regeneration of spent activated carbon obtained from home filtration system and applying it for heavy metals adsorption. J. Environ. Chem. Eng. 5, 3091–3099.

Dai, Y.J., Liu, M., Li, J.J., Yang, S.S., Sun, Y., Sun, Q.Y., Wang, W.S., Lu, L., Zhang, K.X., Xu, J.Y., Zheng, W.L., Hu, Z.Y., Yang, Y.H., Gao, Y.W., Liu, Z.H., 2020. A review on pollution situation and treatment methods of tetracycline in groundwater. Sep. Sci. Technol. 55, 1005–1021.
Dalai, C., Jha, R., Desai, V.R., 2015. Rice husk and sugarcane baggase based activated carbon for iron and manganese removal. Aquat. Procedia 4, 1126–1133.
Darweesh, T.M., Ahmed, M.J., 2017. Batch and fixed bed adsorption of levofloxacin on granular activated carbon from date (*Phoenix dactylifera* L.) stones by KOH chemical activation. Environ. Toxicol. Pharmacol. 50, 159–166.
Das, S., Mishra, S., 2020. Insight into the isotherm modelling, kinetic and thermodynamic exploration of iron adsorption from aqueous media by activated carbon developed from *Limonia acidissima* shell. Mater. Chem. Phys. 245, 122751.
David, E., Kopac, J., 2014. Activated carbons derived from residual biomass pyrolysis and their $CO_2$ adsorption capacity. J. Anal. Appl. Pyrolysis 110, 322–332.
Debnath, D., Gupta, A.K., Ghosal, P.S., 2019. Recent advances in the development of tailored functional materials for the treatment of pesticides in aqueous media: a review. J. Ind. Eng. Chem. 70, 51–69.
Deng, S.B., Nie, Y., Du, Z.W., Huang, Q., Meng, P.P., Wang, B., Huang, J., Yu, G., 2015. Enhanced adsorption of perfluorooctane sulfonate and perfluorooctanoate by bamboo-derived granular activated carbon. J. Hazard. Mater. 282, 150–157.
Deshannavar, U.B., Hegde, P.G., Dhalayat, Z., Patil, V., Gavas, S., 2018. Production and characterization of agro-based briquettes and estimation of calorific value by regression analysis: an energy application. Mater. Sci. Energy Technol. 1, 175–181.
Dias, J.M., Alvim-Ferraz, M.C.M., Almeida, M.F., Rivera-Utrilla, J., Sánchez-Polo, M., 2007. Waste materials for activated carbon preparation and its use in aqueous-phase treatment: a review. J. Environ. Manag. 85, 833–846.
Dong, H.Y., Xu, L., Mao, Y.X., Wang, Y., Duan, S.L., Lian, J.F., Li, J., Yu, J.W., Qiang, Z.M., 2021. Effective abatement of 29 pesticides in full-scale advanced treatment processes of drinking water: from concentration to human exposure risk. J. Hazard. Mater. 403, 123986.
Dong, L.H., Hou, L.A., Wang, Z.S., Gu, P., Chen, G.Y., Jiang, R.F., 2018. A new function of spent activated carbon in BAC process: removing heavy metals by ion exchange mechanism. J. Hazard. Mater. 359, 76–84.
Dong, L.H., Liu, W.J., Yu, Y., Hou, L.A., Gu, P., Chen, G.Y., 2019. Preparation, characterization, and application of macroporous activated carbon (MAC) suitable for the BAC water treatment process. Sci. Total Environ. 647, 1359–1367.
Duan, X.H., Zhang, C.C., Srinivasakannan, C., Wang, X., 2017. Waste walnut shell valorization to iron loaded biochar and its application to arsenic removal. Resour. Effic. Technol. 3, 29–36.
Dzigbor, A., Chimphango, A., 2019. Production and optimization of NaCl-activated carbon from mango seed using response surface methodology. Biomass Convers. Biorefinery 9, 421–431.
Eeshwarasinghe, D., Loganathan, P., Vigneswaran, S., 2019. Simultaneous removal of polycyclic aromatic hydrocarbons and heavy metals from water using granular activated carbon. Chemosphere 223, 616–627.
Egirani, D.E., Poyi, N.R., Shehata, N., 2020. Preparation and characterization of powdered and granular activated carbon from Palmae biomass for cadmium removal. Int. J. Environ. Sci. Technol. 17, 2443–2454.
El Gamal, M., Mousa, H.A., El-Naas, M.H., Zacharia, R., Judd, S., 2018. Bio-regeneration of activated carbon: a comprehensive review. Sep. Purif. Technol. 197, 345–359.
El Mouchtari, E.M., de Daou, C., Rafqah, S., Najjar, F., Anane, H., Piram, A., Hamade, A., Briche, S., Wong-Wah-chung, P., 2020. $TiO_2$ and activated carbon of *Argania* Spinosa tree nutshells composites for the adsorption photocatalysis removal of pharmaceuticals from aqueous solution. J. Photochem. Photobiol. A: Chem. 388, 112183.
Ellison, C.R., Hoff, R., Mărculescu, C., Boldor, D., 2020. Investigation of microwave-assisted pyrolysis of biomass with char in a rectangular waveguide applicator with built-in phase-shifting. Appl. Energy 259, 114217.
Foo, K.Y., Hameed, B.H., 2010. Detoxification of pesticide waste via activated carbon adsorption process. J. Hazard. Mater. 175, 1–11.
Foo, K.Y., Hameed, B.H., 2011. Preparation and characterization of activated carbon from sunflower seed oil residue via microwave assisted $K_2CO_3$ activation. Bioresour. Technol. 102, 9794–9799.
Foo, K.Y., Hameed, B.H., 2012a. Textural porosity, surface chemistry and adsorptive properties of durian shell derived activated carbon prepared by microwave assisted NaOH activation. Chem. Eng. J. 187, 53–62.
Foo, K.Y., Hameed, B.H., 2012b. Porous structure and adsorptive properties of pineapple peel based activated carbons prepared via microwave assisted KOH and $K_2CO_3$ activation. Microporous Mesoporous Mater. 148, 191–195.
Foo, K.Y., Hameed, B.H., 2013. Utilization of oil palm biodiesel solid residue as renewable sources for preparation of granular activated carbon by microwave induced KOH activation. Bioresour. Technol. 130, 696–702.
Fortin, S., Song, B., Burbage, C., 2019. Quantifying and identifying microplastics in the effluent of advanced wastewater treatment systems using Raman microspectroscopy. Mar. Pollut. Bull. 149, 110579.
Fu, J., Lee, W.N., Coleman, C., Nowack, K., Carter, J., Huang, C.H., 2017a. Removal of disinfection byproduct (DBP) precursors in water by two-stage biofiltration treatment. Water Res. 123, 224–235.
Fu, K.F., Yue, Q.Y., Gao, B.Y., Wang, Y., Li, Q., 2017b. Activated carbon from tomato stem by chemical activation with $FeCl_2$. Colloids Surfaces A: Physicochem. Eng. Aspects 529, 842–849.
Fu, Y.H., Zhang, N.Y., Shen, Y.F., Ge, X.L., Chen, M.D., 2018. Micro-mesoporous carbons from original and pelletized rice husk via one-step catalytic pyrolysis. Bioresour. Technol. 269, 67–73.
Gajera, Z.R., Verma, K., Tekade, S.P., Sawarkar, A.N., 2020. Kinetics of co-gasification of rice husk biomass and high sulphur petroleum coke with oxygen as gasifying medium via TGA. Bioresour. Technol. Rep. 11, 100479.
Galvão, R.B., da Silva Moretti, A.A., Fernandes, F., Kuroda, E.K., 2020. Post-treatment of stabilized landfill leachate by upflow gravel filtration and granular activated carbon adsorption. Environ. Technol. 2020, 1–10.
Ganguly, P., Sarkhel, R., Das, P., 2020. Synthesis of pyrolyzed biochar and its application for dye removal: batch, kinetic and isotherm with linear and non-linear mathematical analysis. Surf. Interf. 20, 100616.
Ganji, M.D., Fereidoon, A., Jahanshahi, M., Ghorbanzadeh Ahangari, M., 2012. Elastic properties of SWCNTs with curved morphology: density functional tight binding based treatment. Solid State Commun 152, 1526–1530.
Garg, D., Kumar, S., Sharma, K., Majumder, C.B., 2019. Application of waste peanut shells to form activated carbon and its utilization for the removal of Acid Yellow 36 from wastewater. Groundw. Sustain. Dev. 8, 512–519.
Gebresemati, M., Gabbiye, N., Sahu, O., 2017. Sorption of cyanide from aqueous medium by coffee husk: response surface methodology. J. Appl. Res. Technol. 15, 27–35.
Gebrewold, B.D., Kijjanapanich, P., Rene, E.R., Lens, P.N.L., Annachhatre, A.P., 2019. Fluoride removal from groundwater using chemically modified rice husk and corn cob activated carbon. Environ. Technol. 40, 2913–2927.
Ghorbani, F., Kamari, S., Zamani, S., Akbari, S., Salehi, M., 2020. Optimization and modeling of aqueous Cr(VI) adsorption onto activated carbon prepared from sugar beet bagasse agricultural waste by application of response surface methodology. Surf. Interf. 18, 100444.
Giraldo, L., Moreno-Piraján, J.C., 2012. Synthesis of activated carbon mesoporous from coffee waste and its application in adsorption zinc and mercury ions from aqueous solution. E-J. Chem. 9, 938–948.
Golea, D.M., Jarvis, P., Jefferson, B., Moore, G., Sutherland, S., Parsons, S.A., Judd, S.J., 2020. Influence of granular activated carbon media properties on natural organic matter and disinfection by-product precursor removal from drinking water. Water Res. 174, 115613.
Golea, D.M., Upton, A., Jarvis, P., Moore, G., Sutherland, S., Parsons, S.A., Judd, S.J., 2017. THM and HAA formation from NOM in raw and treated surface waters. Water Res. 112, 226–235.
Gonçalves, G.D.C., Nakamura, P.K., Furtado, D.F., Veit, M.T., 2017. Utilization of brewery residues to produces granular activated carbon and bio-oil. J. Clean. Prod. 168, 908–916.
Gonçalves, G.D.C., Pereira, N.C., Veit, M.T., 2016. Production of bio-oil and activated carbon from sugarcane bagasse and molasses. Biomass Bioenergy 85, 178–186.

Gonçalves, M., Castro, C.S., Boas, I.K.V., Soler, F.C., Pinto, E.D.C., Lavall, R.L., Carvalho, W.A., 2019. Glycerin waste as sustainable precursor for activated carbon production: adsorption properties and application in supercapacitors. J. Environ. Chem. Eng. 7, 103059.
González-García, P., 2018. Activated carbon from lignocellulosics precursors: a review of the synthesis methods, characterization techniques and applications. Renew. Sustain. Energy Rev. 82, 1393–1414.
Guo, G.F., Zhang, K., Liu, C.X., Xie, S.L., Li, X., Li, B., Shu, J.S., Niu, Y., Zhu, H.F., Ding, M.Z., Zhu, W.K., 2020. Comparative investigation on thermal decomposition of powdered and pelletized biomasses: thermal conversion characteristics and apparent kinetics. Bioresour. Technol. 301, 122732.
Gupta, A., Thengane, S.K., Mahajani, S., 2020. Kinetics of pyrolysis and gasification of cotton stalk in the central parts of India. Fuel 263, 116752.
Gurevich Messina, L.I., Bonelli, P.R., Cukierman, A.L., 2017. Effect of acid pretreatment and process temperature on characteristics and yields of pyrolysis products of peanut shells. Renew. Energy 114, 697–707.
Hamad, B.K., 2015. Preparation and characterization of activated carbon from oil palm shell activated by KOH. J. Pure Appl. Sci. 27, 27–28.
Hamed Mashhadzadeh, A., Ghorbanzadeh Ahangari, M., Salmankhani, A., Fataliyan, M., 2018. Density functional theory study of adsorption properties of non-carbon, carbon and functionalized graphene surfaces towards the zinc and lead atoms. Phys. E: Low-Dimensional Syst. 104, 275–285 Nanostructures.
Hao, M.J., Qiu, M.Q., Yang, H., Hu, B.W., Wang, X.X., 2021. Recent advances on preparation and environmental applications of MOF-derived carbons in catalysis. Sci. Total. Environ. 760, 143333.
Hejazifar, M., Azizian, S., Sarikhani, H., Li, Q., Zhao, D.Y., 2011. Microwave assisted preparation of efficient activated carbon from grapevine rhytidome for the removal of methyl violet from aqueous solution. J. Anal. Appl. Pyrolysis 92, 258–266.
Hernández, A.M., Labady, M., Laine, J., 2014. Granular activated carbon from wood originated from tropical virgin forest. Open J. For. 4, 208–211.
Hoseinzadeh Hesas, R., Arami-Niya, A., Wan Daud, W.M.A., Sahu, J.N., 2013. Preparation of granular activated carbon from oil palm shell by microwave-induced chemical activation: optimisation using surface response methodology. Chem. Eng. Res. Des. 91, 2447–2456.
Hossain, N., Bhuiyan, M.A., Pramanik, B.K., Nizamuddin, S., Griffin, G., 2020. Waste materials for wastewater treatment and waste adsorbents for biofuel and cement supplement applications: a critical review. J. Clean. Prod. 255, 120261.
Hou, J.F., Xu, D.L., Li, J., Sun, J.Y., Zheng, S.R., 2020. Enhanced adsorption of o-phenylphenol on zeolites: a combing pore filling and hydrophobic effects. Microporous Mesoporous Mater. 294, 109860.
Hou, L.Y., Kumar, D., Yoo, C.G., Gitsov, I., Majumder, E.L.W., 2021. Conversion and removal strategies for microplastics in wastewater treatment plants and landfills. Chem. Eng. J. 406, 126715.
Hu, B.C., Gao, Z.S., Wang, H.X., Wang, J., Cheng, M.S., 2020. Computational insights into the sorption mechanism of polycyclic aromatic hydrocarbons by carbon nanotube through density functional theory calculation and molecular dynamics simulation. Comput. Mater. Sci. 179, 109677.
Hu, J.L., Chu, W.H., Sui, M.H., Xu, B., Gao, N.Y., Ding, S.K., 2018. Comparison of drinking water treatment processes combinations for the minimization of subsequent disinfection by-products formation during chlorination and chloramination. Chem. Eng. J. 335, 352–361.
Hu, Q., Shao, J.G., Yang, H.P., Yao, D.D., Wang, X.H., Chen, H.P., 2015. Effects of binders on the properties of bio-char pellets. Appl. Energy 157, 508–516.
Hu, Q., Yang, H.P., Yao, D.D., Zhu, D.C., Wang, X.H., Shao, J.G., Chen, H.P., 2016. The densification of bio-char: effect of pyrolysis temperature on the qualities of pellets. Bioresour. Technol. 200, 521–527.
Huang, N., Zhao, P.T., Ghosh, S., Fedyukhin, A., 2019. Co-hydrothermal carbonization of polyvinyl chloride and moist biomass to remove chlorine and inorganics for clean fuel production. Appl. Energy 240, 882–892.
Huang, Y.F., MacKenzie, A., Meteer, L., Hofmann, R., 2020. Evaluation of phosphorus removal from a lake by two drinking water treatment plants. Environ. Technol. 41, 863–869.
Huggins, T.M., Haeger, A., Biffinger, J.C., Ren, Z.J., 2016. Granular biochar compared with activated carbon for wastewater treatment and resource recovery. Water Res 94, 225–232.
Ideta, K., Kim, D.W., Kim, T., Nakabayashi, K., Miyawaki, J., Park, J.I., Yoon, S.H., 2020. 19F ex situ solid-state NMR study on structural differences in pores of activated carbon series derived from chemical and physical activation processes for EDLCs. J. Phys. Chem. C 124, 12457–12465.
Iftikhar, M., Asghar, A., Ramzan, N., Sajjadi, B., Chen, W.Y., 2019. Biomass densification: effect of cow dung on the physicochemical properties of wheat straw and rice husk based biomass pellets. Biomass Bioenergy 122, 1–16.
Ighalo, J.O., Adeniyi, A.G., Adelodun, A.A., 2021. Recent advances on the adsorption of herbicides and pesticides from polluted waters: performance evaluation via physical attributes. J. Ind. Eng. Chem. 93, 117–137.
Islam, M.S., Rouf, M.A., 2013. Waste biomass as sources for activated carbon production: a review. Bangladesh J. Sci. Ind. Res. 47, 347–364.
Islam, N.F., Sarma, H., Prasad, M.N., 2020. Emerging Disinfection By-Products in water: Novel Biofiltration techniques. Disinfection By-Products in Drinking Water. Elsevier, Amsterdam, pp. 109–135.
Jain, A., Xu, C.H., Jayaraman, S., Balasubramanian, R., Lee, J.Y., Srinivasan, M.P., 2015. Mesoporous activated carbons with enhanced porosity by optimal hydrothermal pre-treatment of biomass for supercapacitor applications. Microporous Mesoporous Mater 218, 55–61.
Janković, B., Manić, N., Dodevski, V., Radović, I., Pijović, M., Katnić, Đ., Tasić, G., 2019. Physico-chemical characterization of carbonized apricot kernel shell as precursor for activated carbon preparation in clean technology utilization. J. Clean. Prod. 236, 117614.
Jaria, G., Calisto, V., Silva, C.P., Gil, M.V., Otero, M., Esteves, V.I., 2019. Obtaining granular activated carbon from paper mill sludge: a challenge for application in the removal of pharmaceuticals from wastewater. Sci. Total. Environ. 653, 393–400.
Jiang, J.Y., Zhang, X.R., 2018. A smart strategy for controlling disinfection byproducts by reversing the sequence of activated carbon adsorption and chlorine disinfection. Sci. Bull. 63, 1167–1169.
Jiang, J.Y., Zhang, X.R., Zhu, X.H., Li, Y., 2017. Removal of intermediate aromatic halogenated DBPs by activated carbon adsorption: a new approach to controlling halogenated DBPs in chlorinated drinking water. Environ. Sci. Technol. 51, 3435–3444.
Jiang, X.C., Guo, F.Q., Jia, X.P., Zhan, Y.B., Zhou, H.M., Qian, L., 2020. Synthesis of nitrogen-doped hierarchical porous carbons from peanut shell as a promising electrode material for high-performance supercapacitors. J. Energy Storage 30, 101451.
Jin, E., Lee, S., Kang, E., Kim, Y., Choe, W., 2020. Metal-organic frameworks as advanced adsorbents for pharmaceutical and personal care products. Coord. Chem. Rev. 425, 213526.
Jung, K.W., Choi, B.H., Hwang, M.J., Jeong, T.U., Ahn, K.H., 2016. Fabrication of granular activated carbons derived from spent coffee grounds by entrapment in calcium alginate beads for adsorption of acid orange 7 and methylene blue. Bioresour. Technol. 219, 185–195.
Jusoh, A., Hartini, W.J.H., Ali, N., Endut, A., 2011. Study on the removal of pesticide in agricultural run off by granular activated carbon. Bioresour. Technol. 102, 5312–5318.
Kalaruban, M., Loganathan, P., Nguyen, T.V., Nur, T., Hasan Johir, M.A., Nguyen, T.H., Trinh, M.V., Vigneswaran, S., 2019. Iron-impregnated granular activated carbon for arsenic removal: application to practical column filters. J. Environ. Manag. 239, 235–243.
Kalderis, D., Bethanis, S., Paraskeva, P., Diamadopoulos, E., 2008a. Production of activated carbon from bagasse and rice husk by a single-stage chemical activation method at low retention times. Bioresour. Technol. 99, 6809–6816.
Kalderis, D., Koutoulakis, D., Paraskeva, P., Diamadopoulos, E., Otal, E., Valle, J.O.D., Fernández-Pereira, C., 2008b. Adsorption of polluting substances on activated carbons prepared from rice husk and sugarcane bagasse. Chem. Eng. J. 144, 42–50.
Kan, Y., Yue, Q., Gao, B., Li, Q., 2015. Comparative study of dry-mixing and wet-mixing activated carbons prepared from waste printed circuit boards by NaOH activation. RSC Adv. 5, 105943–105951.
Kan, Y.J., Yue, Q.Y., Li, D., Wu, Y.W., Gao, B.Y., 2017. Preparation and characterization of activated carbons from waste tea by $H_3PO_4$ activation in different atmospheres for oxytetracycline removal. J. Taiwan Inst. Chem. Eng. 71, 494–500.
Kang, K., Nanda, S., Sun, G.T., Qiu, L., Gu, Y.Q., Zhang, T.L., Zhu, M.Q., Sun, R.C., 2019. Microwave-assisted hydrothermal carbonization of corn stalk for solid biofuel production: optimization of process parameters and characterization of hydrochar. Energy 186, 115795.
Kårelid, V., Larsson, G., Björlenius, B., 2017. Pilot-scale removal of pharmaceuticals in municipal wastewater: comparison of granular and powdered activated carbon treatment at three wastewater treatment plants. J. Environ. Manag. 193, 491–502.

Karri, R.R., Sahu, J.N., Meikap, B.C., 2020. Improving efficacy of Cr(VI) adsorption process on sustainable adsorbent derived from waste biomass (sugarcane bagasse) with help of ant colony optimization. Ind. Crop. Prod. 143, 111927.
Kaur, M., Neetu, Pal Verma, Y., Chauhan, S., 2020. Effect of chemical pretreatment of sugarcane bagasse on biogas production. Mater. Today: Proc 21, 1937–1942.
Kaur, P., Kaur, P., Kaur, K., 2019. Adsorptive removal of imazethapyr and imazamox from aqueous solution using modified rice husk. J. Clean. Prod. 244, 118699.
Khadhri, N., El Khames Saad, M., ben Mosbah, M., Moussaoui, Y., 2019. Batch and continuous column adsorption of indigo carmine onto activated carbon derived from date palm petiole. J. Environ. Chem. Eng. 7, 102775.
Khoshbouy, R., Takahashi, F., Yoshikawa, K., 2019. Preparation of high surface area sludge-based activated hydrochar via hydrothermal carbonization and application in the removal of basic dye. Environ. Res. 175, 457–467.
Kim, K.H., Bai, X.L., Rover, M., Brown, R.C., 2014. The effect of low-concentration oxygen in sweep gas during pyrolysis of red oak using a fluidized bed reactor. Fuel 124, 49–56.
Kim, Y., Bae, J., Park, H., Suh, J.K., You, Y.W., Choi, H., 2016. Adsorption dynamics of methyl violet onto granulated mesoporous carbon: facile synthesis and adsorption kinetics. Water Res 101, 187–194.
Korotta-Gamage, S.M., Sathasivan, A., 2017. A review: potential and challenges of biologically activated carbon to remove natural organic matter in drinking water purification process. Chemosphere 167, 120–138.
Köseoğlu, E., Akmil-Başar, C., 2015. Preparation, structural evaluation and adsorptive properties of activated carbon from agricultural waste biomass. Adv. Powder Technol. 26, 811–818.
Koutník, I., Vráblová, M., Bednárek, J., 2020. *Reynoutria japonica*, an invasive herb as a source of activated carbon for the removal of xenobiotics from water. Bioresour. Technol. 309, 123315.
Kumagai, S., Ishizawa, H., Aoki, Y., Toida, Y., 2010. Molded micro- and mesoporous carbon/silica composite from rice husk and beet sugar. Chem. Eng. J. 156, 270–277.
Kumar, M., Upadhyay, S.N., Mishra, P.K., 2019. A comparative study of thermochemical characteristics of lignocellulosic biomasses. Bioresour. Technol. Rep. 8, 100186.
Kuntail, J., Jain, Y.M., Shukla, M., Sinha, I., 2019. Adsorption mechanism of phenol, p-chlorophenol, and p-nitrophenol on magnetite surface: a molecular dynamics study. J. Mol. Liq. 288, 111053.
Kutluay, S., Baytar, O., Şahin, Ö., 2019. Equilibrium, kinetic and thermodynamic studies for dynamic adsorption of benzene in gas phase onto activated carbon produced from *Elaeagnus angustifolia* seeds. J. Environ. Chem. Eng. 7, 102947.
Kwon, G., Bhatnagar, A., Wang, H.L., Kwon, E.E., Song, H., 2020. A review of recent advancements in utilization of biomass and industrial wastes into engineered biochar. J. Hazard. Mater. 400, 123242.
Larous, S., Meniai, A.H., 2012. The use of sawdust as by product adsorbent of organic pollutant from wastewater: adsorption of phenol. Energy Procedia 18, 905–914.
Lee, J.H., Heo, Y.J., Park, S.J., 2018. Effect of silica removal and steam activation on extra-porous activated carbons from rice husks for methane storage. Int. J. Hydrog. Energy 43, 22377–22384.
Levchuk, I., Rueda Márquez, J.J., Sillanpää, M., 2018. Removal of natural organic matter (NOM) from water by ion exchange: a review. Chemosphere 192, 90–104.
Li, B.S., Liu, Y.X., Li, R.D., Yang, T.H., Kai, X.P., 2020a. Aluminum-water reactions assisted in situ hydrodeoxygenation of enzymolysis lignin from bioconversion of rice straw over NiMo catalyst. Ind. Crop. Prod. 154, 112727.
Li, B.Z., Yang, Y.C., Wu, H.Y., Zhang, C., Zheng, W., Sun, D.K., 2020b. Adsorptive removal and mechanism of monocyclic aromatics by activated carbons from water: effects of structure and surface chemistry. Colloids Surfaces A: Physicochem. Eng. Aspects 605, 125346.
Li, C., Wang, L., Shen, Y.G., 2014. The removal of atrazine, simazine, and prometryn by granular activated carbon in aqueous solution. Desalination Water Treat 52, 3510–3516.
Li, Y.J., Yue, Q.Y., Li, W.H., Gao, B.Y., Li, J.Z., Du, J.D., 2011. Properties improvement of paper mill sludge-based granular activated carbon fillers for fluidized-bed bioreactor by bentonite (Na) added and acid washing. J. Hazard. Mater. 197, 33–39.
Liang, S., Ye, N., Hu, Y.C., Shi, Y.F., Zhang, W., Yu, W.B., Wu, X., Yang, J.K., 2016. Lead adsorption from aqueous solutions by a granular adsorbent prepared from *Phoenix* tree leaves. RSC Adv 6, 25393–25400.
Lima, L., Baêta, B.E.L., Lima, D.R.S., Afonso, R.J.C.F., de Aquino, S.F., Libânio, M., 2016. Comparison between two forms of granular activated carbon for the removal of pharmaceuticals from different waters. Environ. Technol. 37, 1334–1345.
Liu, D.Q., Xie, Q., Huang, X.Q., Wan, C.R., Deng, F., Liang, D.C., Liu, J.C., 2020a. Backwashing behavior and hydrodynamic performances of granular activated carbon blends. Environ. Res. 184, 109302.
Liu, L.H., Lin, Y., Liu, Y.Y., He, Q., 2014. Effect of binders on porous properties, surface chemical properties and adsorption characteristics of granular adsorbents from sewage sludge. Mater. Sci. 20, 488–492.
Liu, M.P., Zhu, L., Zhang, X.X., Han, W.H., Qiu, Y.P., 2020b. Insight into the role of ion-pairing in the adsorption of imidazolium derivative-based ionic liquids by activated carbon. Sci. Total. Environ. 743, 140644.
Lu, Z.D., Sun, W.J., Li, C., Cao, W.F., Jing, Z.B., Li, S.M., Ao, X.W., Chen, C., Liu, S.M., 2020. Effect of granular activated carbon pore-size distribution on biological activated carbon filter performance. Water Res 177, 115768.
Lütke, S.F., Igansi, A.V., Pegoraro, L., Dotto, G.L., Pinto, L.A.A., Cadaval Jr, T.R.S., 2019. Preparation of activated carbon from black wattle bark waste and its application for phenol adsorption. J. Environ. Chem. Eng. 7, 103396.
Ma, Q.L., Han, L.J., Huang, G.Q., 2018. Effect of water-washing of wheat straw and hydrothermal temperature on its hydrochar evolution and combustion properties. Bioresour. Technol. 269, 96–103.
Mailler, R., Gasperi, J., Coquet, Y., Derome, C., Buleté, A., Vulliet, E., Bressy, A., Varrault, G., Chebbo, G., Rocher, V., 2016. Removal of emerging micropollutants from wastewater by activated carbon adsorption: experimental study of different activated carbons and factors influencing the adsorption of micropollutants in wastewater. J. Environ. Chem. Eng. 4, 1102–1109.
Mallek, M., Chtourou, M., Portillo, M., Monclús, H., Walha, K., Salah, A.B., Salvadó, V., 2018. Granulated cork as biosorbent for the removal of phenol derivatives and emerging contaminants. J. Environ. Manag. 223, 576–585.
Martínez, L.V., Rubiano, J.E., Figueredo, M., Gómez, M.F., 2020. Experimental study on the performance of gasification of corncobs in a downdraft fixed bed gasifier at various conditions. Renew. Energy 148, 1216–1226.
Martín-Lara, M.A., Pérez, A., Vico-Pérez, M.A., Calero, M., Blázquez, G., 2019. The role of temperature on slow pyrolysis of olive cake for the production of solid fuels and adsorbents. Process. Saf. Environ. Prot. 121, 209–220.
Mason, S.A., Welch, V.G., Neratko, J., 2018. Synthetic polymer contamination in bottled water. Front. Chem. 6, 407.
Masoumi, S., Dalai, A.K., 2020. Optimized production and characterization of highly porous activated carbon from algal-derived hydrochar. J. Clean. Prod. 263, 121427.
Matilainen, A., Gjessing, E.T., Lahtinen, T., Hed, L., Bhatnagar, A., Sillanpää, M., 2011. An overview of the methods used in the characterisation of natural organic matter (NOM) in relation to drinking water treatment. Chemosphere 83, 1431–1442.
Matilainen, A., Vieno, N., Tuhkanen, T., 2006. Efficiency of the activated carbon filtration in the natural organic matter removal. Environ. Int. 32, 324–331.
Matsushita, T., Morimoto, A., Kuriyama, T., Matsumoto, E., Matsui, Y., Shirasaki, N., Kondo, T., Takanashi, H., Kameya, T., 2018. Removals of pesticides and pesticide transformation products during drinking water treatment processes and their impact on mutagen formation potential after chlorination. Water Res 138, 67–76.
Meinel, F., Ruhl, A.S., Sperlich, A., Zietzschmann, F., Jekel, M., 2014. Pilot-scale investigation of micropollutant removal with granular and powdered activated carbon. Water Air Soil Pollut 226, 1–10.
Menya, E., Olupot, P.W., Storz, H., Lubwama, M., Kiros, Y., 2018. Production and performance of activated carbon from rice husks for removal of natural organic matter from water: a review. Chem. Eng. Res. Des. 129, 271–296.
Menya, E., Olupot, P.W., Storz, H., Lubwama, M., Kiros, Y., 2020. Synthesis and evaluation of activated carbon from rice husks for removal of humic acid from water. Biomass Convers. Biorefin. 1–20.

Mintenig, S.M., Löder, M.G.J., Primpke, S., Gerdts, G., 2019. Low numbers of microplastics detected in drinking water from ground water sources. Sci. Total. Environ. 648, 631–635.
Missagia, B., Guerrero, C., Narra, S., Sun, Y.L., Ay, P., Krautz, H.J., 2011. Physicomechanical properties of rice husk pellets for energy generation. Energy Fuels 25, 5786–5790.
Missaoui, A., Bostyn, S., Belandria, V., Cagnon, B., Sarh, B., Gökalp, I., 2017. Hydrothermal carbonization of dried olive pomace: energy potential and process performances. J. Anal. Appl. Pyrolysis 128, 281–290.
Mohamad Nor, N., Lau, L.C., Lee, K.T., Mohamed, A.R., 2013. Synthesis of activated carbon from lignocellulosic biomass and its applications in air pollution control—A review. J. Environ. Chem. Eng. 1, 658–666.
Mohamed, M.A., Jaafar, J., Ismail, A.F., Othman, M.H.D., Rahman, M.A., 2017. Fourier Transform Infrared (FTIR) spectroscopy. Membrane Characterization. Elsevier, Amsterdam, pp. 3–29.
Mohammed, I.Y., Abakr, Y.A., Musa, M., Yusup, S., Singh, A., Kazi, F.K., 2016. Valorization of *Bambara* groundnut shell via intermediate pyrolysis: products distribution and characterization. J. Clean. Prod. 139, 717–728.
Mohd Faizal, H., Shamsuddin, H.S., M. Heiree, M.H., Muhammad Ariff Hanaffi, M.F., Abdul Rahman, M.R., Rahman, M.M., Latiff, Z.A., 2018. Torrefaction of densified mesocarp fibre and palm kernel shell. Renew. Energy 122, 419–428.
Muazu, R.I., Stegemann, J.A., 2015. Effects of operating variables on durability of fuel briquettes from rice husks and corn cobs. Fuel Process. Technol. 133, 137–145.
Mustafa, R., Asmatulu, E., 2020. Preparation of activated carbon using fruit, paper and clothing wastes for wastewater treatment. J. Water Process. Eng. 35, 101239.
Myers, M.A., Johnson, N.W., Marin, E.Z., Pornwongthong, P., Liu, Y., Gedalanga, P.B., Mahendra, S., 2018. Abiotic and bioaugmented granular activated carbon for the treatment of 1, 4-dioxane-contaminated water. Environ. Pollut. 240, 916–924.
Nagalakshmi, T.V., Emmanuel, K.A., Bhavani, P., 2019. Adsorption of disperse blue 14 onto activated carbon prepared from Jackfruit-PPI-I waste. Mater. Today: Proc. 18, 2036–2051.
Naqvi, S.R., Ali, I., Nasir, S., Ali Ammar Taqvi, S., Atabani, A.E., Chen, W.H., 2020. Assessment of agro-industrial residues for bioenergy potential by investigating thermo-kinetic behavior in a slow pyrolysis process. Fuel 278, 118259.
Nasri, N.S., Zain, H.M., D.Usman, H., Majid, Z.A., Sharer, Z., Sazali, N.A., Anirman, N.L., 2013. $CO_2$ adsorption-breakthrough study on activated carbon derived from renewable oil palm empty fruit bunch. Aust. J. Basic Appl. Sci. 7, 222–231.
Nawaz, T., Sengupta, S., 2019. Contaminants of Emerging concern: occurrence, fate, and remediation. Advances in Water Purification Techniques. Elsevier, Amsterdam, pp. 67–114.
Nguyen, D.T., Tran, H.N., Juang, R.S., Dat, N.D., Tomul, F., Ivanets, A., Woo, S.H., Hosseini-Bandegharaei, A., Nguyen, V.P., Chao, H.P., 2020. Adsorption process and mechanism of acetaminophen onto commercial activated carbon. J. Environ. Chem. Eng. 8, 104408.
Nieto-Delgado, C., Terrones, M., Rangel-Mendez, J.R., 2011. Development of highly microporous activated carbon from the alcoholic beverage industry organic by-products. Biomass Bioenergy 35, 103–112.
Nikić, J., Agbaba, J., Watson, M.A., Tubić, A., Šolić, M., Maletić, S., Dalmacija, B., 2019. Arsenic adsorption on Fe-Mn modified granular activated carbon (GAC-FeMn): batch and fixed-bed column studies. J. Environ. Sci. Heal. 54, 168–178.
Njoku, V.O., Foo, K.Y., Hameed, B.H., 2013. Microwave-assisted preparation of pumpkin seed hull activated carbon and its application for the adsorptive removal of 2, 4-dichlorophenoxyacetic acid. Chem. Eng. J. 215/216, 383–388.
Njoku, V.O., Islam, M.A., Asif, M., Hameed, B.H., 2015. Adsorption of 2, 4-dichlorophenoxyacetic acid by mesoporous activated carbon prepared from $H_3PO_4$-activated langsat empty fruit bunch. J. Environ. Manag. 154, 138–144.
Norouzi, S., Heidari, M., Alipour, V., Rahmanian, O., Fazlzadeh, M., Mohammadi-Moghadam, F., Nourmoradi, H., Goudarzi, B., Dindarloo, K., 2018. Preparation, characterization and Cr(VI) adsorption evaluation of NaOH-activated carbon produced from Date Press Cake; an agro-industrial waste. Bioresour. Technol. 258, 48–56.
Novotna, K., Cermakova, L., Pivokonska, L., Cajthaml, T., Pivokonsky, M., 2019. Microplastics in drinking water treatment—Current knowledge and research needs. Sci. Total. Environ. 667, 730–740.
Nunell, G.V., Fernández, M.E., Bonelli, P.R., Cukierman, A.L., 2012. Conversion of biomass from an invasive species into activated carbons for removal of nitrate from wastewater. Biomass Bioenergy 44, 87–95.
Ogata, F., Tominaga, H., Yabutani, H., Taga, A., Kawasaki, N., 2012. Granulation of gibbsite with inorganic binder and its ability to adsorb Mo(VI) from aqueous solution. Toxicol. Environ. Chem. 94, 650–659.
Olupot, P.W., Candia, A., Menya, E., Walozi, R., 2016. Characterization of rice husk varieties in *Uganda* for biofuels and their techno-economic feasibility in gasification. Chem. Eng. Res. Des. 107, 63–72.
Omorogie, M.O., Naidoo, E.B., Ofomaja, A.E., 2017. Response surface methodology, central composite design, process methodology and characterization of pyrolyzed KOH pretreated environmental biomass: mathematical modelling and optimization approach. Model. Earth Syst. Environ. 3, 1171–1186.
Oßmann, B.E., Sarau, G., Holtmannspötter, H., Pischetsrieder, M., Christiansen, S.H., Dicke, W., 2018. Small-sized microplastics and pigmented particles in bottled mineral water. Water Res 141, 307–316.
Ouyang, J.B., Zhou, L.M., Liu, Z.R., Heng, J.Y.Y., Chen, W.Q., 2020. Biomass-derived activated carbons for the removal of pharmaceutical mircopollutants from wastewater: a review. Sep. Purif. Technol. 253, 117536.
Ozbay, N., Yargic, A.S., Yarbay Sahin, R.Z., Yaman, E., 2019. Valorization of banana peel waste via in situ catalytic pyrolysis using Al-Modified SBA-15. Renew. Energy 140, 633–646.
Özdemir, M., Bolgaz, T., Saka, C., Şahin, Ö., 2011. Preparation and characterization of activated carbon from cotton stalks in a two-stage process. J. Anal. Appl. Pyrolysis 92, 171–175.
Palansooriya, K.N., Yang, Y., Tsang, Y.F., Sarkar, B., Hou, D.Y., Cao, X.D., Meers, E., Rinklebe, J., Kim, K.H., Ok, Y.S., 2020. Occurrence of contaminants in drinking water sources and the potential of biochar for water quality improvement: a review. Crit. Rev. Environ. Sci. Technol. 50, 549–611.
Pallarés, J., González-Cencerrado, A., Arauzo, I., 2018. Production and characterization of activated carbon from barley straw by physical activation with carbon dioxide and steam. Biomass Bioenergy 115, 64–73.
Paredes, L., Fernandez-Fontaina, E., Lema, J.M., Omil, F., Carballa, M., 2016. Understanding the fate of organic micropollutants in sand and granular activated carbon biofiltration systems. Sci. Total. Environ. 551/552, 640–648.
Park, K.Y., Yu, Y.J., Yun, S.J., Kweon, J.H., 2019. Natural organic matter removal from algal-rich water and disinfection by-products formation potential reduction by powdered activated carbon adsorption. J. Environ. Manag. 235, 310–318.
Pathak, P.D., Mandavgane, S.A., 2015. Preparation and characterization of raw and carbon from banana peel by microwave activation: application in citric acid adsorption. J. Environ. Chem. Eng. 3, 2435–2447.
Patowary, D., Baruah, D.C., 2018. Effect of combined chemical and thermal pretreatments on biogas production from lignocellulosic biomasses. Ind. Crop. Prod. 124, 735–746.
Pesqueira, J.F.J.R., Pereira, M.F.R., Silva, A.M.T., 2020. Environmental impact assessment of advanced urban wastewater treatment technologies for the removal of priority substances and contaminants of emerging concern: a review. J. Clean. Prod. 261, 121078.
Piai, L., Blokland, M., van der Wal, A., Langenhoff, A., 2020. Biodegradation and adsorption of micropollutants by biological activated carbon from a drinking water production plant. J. Hazard. Mater. 388, 122028.
Piai, L., Dykstra, J.E., Adishakti, M.G., Blokland, M., Langenhoff, A.A.M., van der Wal, A., 2019. Diffusion of hydrophilic organic micropollutants in granular activated carbon with different pore sizes. Water Res 162, 518–527.
Pivokonsky, M., Cermakova, L., Novotna, K., Peer, P., Cajthaml, T., Janda, V., 2018. Occurrence of microplastics in raw and treated drinking water. Sci. Total Environ. 643, 1644–1651.
Pivokonský, M., Pivokonská, L., Novotná, K., Čermáková, L., Klimtová, M., 2020. Occurrence and fate of microplastics at two different drinking water treatment plants within a river catchment. Sci. Total Environ. 741, 140236.

Plaza, M.G., Durán, I., Rubiera, F., Pevida, C., 2015. $CO_2$ adsorbent pellets produced from pine sawdust: effect of coal tar pitch addition. Appl. Energy 144, 182–192.
Plaza-Recobert, M., Trautwein, G., Pérez-Cadenas, M., Alcañiz-Monge, J., 2017. Preparation of binderless activated carbon monoliths from cocoa bean husk. Microporous Mesoporous Mater 243, 28–38.
Poinern, G.E.J., Senanayake, G., Shah, N., Thi-Le, X.N., Parkinson, G.M., Fawcett, D., 2011. Adsorption of the aurocyanide, $Au(CN)_2$- complex on granular activated carbons derived from *Macadamia nut* shells—A preliminary study. Miner. Eng. 24, 1694–1702.
Popov, M., Kragulj Isakovski, M., Molnar Jazić, J., Tubić, A., Watson, M., Šćiban, M., Agbaba, J., 2020. Fate of natural organic matter and oxidation/disinfection by-products formation at a full-scale drinking water treatment plant. Environ. Technol. 2020, 1–12.
Qiu, G.N., Guo, M.X., 2010. Quality of poultry litter-derived granular activated carbon. Bioresour. Technol. 101, 379–386.
Rajput, S.P., Jadhav, S.V., Thorat, B.N., 2020. Methods to improve properties of fuel pellets obtained from different biomass sources: effect of biomass blends and binders. Fuel Process. Technol. 199, 106255.
Rashidi, N.A., Yusup, S., 2017. A review on recent technological advancement in the activated carbon production from oil palm wastes. Chem. Eng. J. 314, 277–290.
Rizhikovs, J., Zandersons, J., Spince, B., Dobele, G., Jakab, E., 2012. Preparation of granular activated carbon from hydrothermally treated and pelletized deciduous wood. J. Anal. Appl. Pyrolysis 93, 68–76.
Saeidi, N., Lotfollahi, M.N., 2015. Effects of powder activated carbon particle size on activated carbon monolith's properties. Mater. Manuf. Process. 31, 1634–1638.
Saha, S., Kurade, M.B., El-Dalatony, M.M., Chatterjee, P.K., Lee, D.S., Jeon, B.H., 2016. Improving bioavailability of fruit wastes using organic acid: an exploratory study of biomass pretreatment for fermentation. Energy Convers. Manag. 127, 256–264.
Sajjadi, S.A., Meknati, A., Lima, E.C., Dotto, G.L., Mendoza-Castillo, D.I., Anastopoulos, I., Alakhras, F., Unuabonah, E.I., Singh, P., Hosseini-Bandegharaei, A., 2019. A novel route for preparation of chemically activated carbon from pistachio wood for highly efficient Pb(II) sorption. J. Environ. Manag. 236, 34–44.
Sajjadi, S.A., Mohammadzadeh, A., Tran, H.N., Anastopoulos, I., Dotto, G.L., Lopičić, Z.R., Sivamani, S., Rahmani-Sani, A., Ivanets, A., Hosseini-Bandegharaei, A., 2018. Efficient mercury removal from wastewater by pistachio wood wastes-derived activated carbon prepared by chemical activation using a novel activating agent. J. Environ. Manag. 223, 1001–1009.
Salman, J.M., 2014. Optimization of preparation conditions for activated carbon from palm oil fronds using response surface methodology on removal of pesticides from aqueous solution. Arab. J. Chem. 7, 101–108.
Salomón-Negrete, M.Á., Reynel-Ávila, H.E., Mendoza-Castillo, D.I., Bonilla-Petriciolet, A., Duran-Valle, C.J., 2018. Water defluoridation with avocado-based adsorbents: synthesis, physicochemical characterization and thermodynamic studies. J. Mol. Liq. 254, 188–197.
Santoso, E., Ediati, R., Kusumawati, Y., Bahruji, H., Sulistiono, D.O., Prasetyoko, D., 2020. Review on recent advances of carbon based adsorbent for methylene blue removal from waste water. Mater. Today Chem. 16, 100233.
Sayğılı, H., Güzel, F., Önal, Y., 2015. Conversion of grape industrial processing waste to activated carbon sorbent and its performance in cationic and anionic dyes adsorption. J. Clean. Prod. 93, 84–93.
Schymanski, D., Goldbeck, C., Humpf, H.U., Fürst, P., 2018. Analysis of microplastics in water by micro-Raman spectroscopy: release of plastic particles from different packaging into mineral water. Water Res 129, 154–162.
Semercioöz, A.S., Göğüş, F., Çelekli, A., Bozkurt, H., 2017. Development of carbonaceous material from grapefruit peel with microwave implemented-low temperature hydrothermal carbonization technique for the adsorption of Cu (II). J. Clean. Prod. 165, 599–610.
Serp, P., Machado, B., 2015. Nanostructured Carbon Materials For Catalysis. Royal Society of Chemistry, UK, pp. 1–45 Nanostructured Carbon Materials for Catalysis.
Setter, C., Silva, F.T.M., Assis, M.R., Ataíde, C.H., Trugilho, P.F., Oliveira, T.J.P., 2020. Slow pyrolysis of coffee husk briquettes: characterization of the solid and liquid fractions. Fuel 261, 116420.
Seyedein Ghannad, S.M.R., Lotfollahi, M.N., 2018. Preparation of granular activated carbons from composite of powder activated carbon and modified $\beta$-zeolite and application to heavy metals removal. Water Sci. Technol. 77, 1591–1601.
Shahabazuddin, M., Sarat Chandra, T., Meena, S., Sukumaran, R.K., Shetty, N.P., Mudliar, S.N., 2018. Thermal assisted alkaline pretreatment of rice husk for enhanced biomass deconstruction and enzymatic saccharification: physico-chemical and structural characterization. Bioresour. Technol. 263, 199–206.
Shaheen, S.M., Niazi, N.K., Hassan, N.E.E., Bibi, I., Wang, H.L., Tsang, D.C.W., Ok, Y.S., Bolan, N., Rinklebe, J., 2019. Wood-based biochar for the removal of potentially toxic elements in water and wastewater: a critical review. Int. Mater. Rev. 64, 216–247.
Shakya, A., Agarwal, T., 2019. Removal of Cr(VI) from water using pineapple peel derived biochars: adsorption potential and re-usability assessment. J. Mol. Liq. 293, 111497.
Shao, Y.C., Tan, H., Shen, D.S., Zhou, Y., Jin, Z.Y., Zhou, D., Lu, W.J., Long, Y.Y., 2020. Synthesis of improved hydrochar by microwave hydrothermal carbonization of green waste. Fuel 266, 117146.
Sharma, R., Jasrotia, K., Singh, N., Ghosh, P., Srivastava, S., Sharma, N.R., Singh, J., Kanwar, R., Kumar, A., 2020. A comprehensive review on hydrothermal carbonization of biomass and its applications. Chem. Afr. 3, 1–19.
Shen, F., Liu, J., Zhang, Z., Dong, Y., Gu, C., 2018. Density functional study of hydrogen sulfide adsorption mechanism on activated carbon. Fuel Process. Technol. 171, 258–264.
Shen, Z.T., Zhang, Y.H., McMillan, O., Jin, F., Al-Tabbaa, A., 2017. Characteristics and mechanisms of nickel adsorption on biochars produced from wheat straw pellets and rice husk. Environ. Sci. Pollut. Res. 24, 12809–12819.
Shin, J., Lee, S.H., Kim, S., Ochir, D., Park, Y., Kim, J., Lee, Y.G., Chon, K., 2020. Effects of physicochemical properties of biochar derived from spent coffee grounds and commercial activated carbon on adsorption behavior and mechanisms of strontium ions (Sr2+). Environ. Sci. Pollut. Res. doi:10.1007/s11356-020-10095-6.
Shruti, V.C., Pérez-Guevara, F., Kutralam-Muniasamy, G., 2020. Metro station free drinking water fountain—A potential "microplastics hotspot" for human consumption. Environ. Pollut. 261. doi:10.1016/j.envpol.2020.114227.
Shukla, N., Sahoo, D., Remya, N., 2019. Biochar from microwave pyrolysis of rice husk for tertiary wastewater treatment and soil nourishment. J. Clean. Prod. 235, 1073–1079.
Si, Y.H., Hu, J.H., Wang, X.H., Yang, H.P., Chen, Y.Q., Shao, J.G., Chen, H.P., 2016. Effect of carboxymethyl cellulose binder on the quality of biomass pellets. Energy Fuels 30, 5799–5808.
Siddiqi, H., Bal, M., Kumari, U., Meikap, B.C., 2020a. In-depth physiochemical characterization and detailed thermo-kinetic study of biomass wastes to analyze its energy potential. Renew. Energy 148, 756–771.
Siddiqi, H., Kumari, U., Biswas, S., Mishra, A., Meikap, B.C., 2020b. A synergistic study of reaction kinetics and heat transfer with multi-component modelling approach for the pyrolysis of biomass waste. Energy 204, 117933.
Sindelar, H.R., Brown, M.T., Boyer, T.H., 2014. Evaluating UV/$H_2O_2$, UV/percarbonate, and UV/perborate for natural organic matter reduction from alternative water sources. Chemosphere 105, 112–118.
Smith, K.M., Fowler, G.D., Pullket, S., Graham, N.J.D., 2012. The production of attrition resistant, sewage-sludge derived, granular activated carbon. Sep. Purif. Technol. 98, 240–248.
Song, X.B., Zhang, S.Y., Wu, Y.M., Cao, Z.Y., 2020. Investigation on the properties of the bio-briquette fuel prepared from hydrothermal pretreated cotton stalk and wood sawdust. Renew. Energy 151, 184–191.
Sun, X.F., Chen, M., Wei, D.B., Du, Y.G., 2019. Research progress of disinfection and disinfection by-products in China. J. Environ. Sci. 81, 52–67.
Supong, A., Bhomick, P.C., Baruah, M., Pongener, C., Sinha, U.B., Sinha, D., 2019. Adsorptive removal of Bisphenol A by biomass activated carbon and insights into the adsorption mechanism through density functional theory calculations. Sustain. Chem. Pharm. 13, 100159.
Talat, M., Mohan, S., Dixit, V., Singh, D.K., Hasan, S.H., Srivastava, O.N., 2018. Effective removal of fluoride from water by coconut husk activated carbon in fixed bed column: experimental and breakthrough curves analysis. Groundw. Sustain. Dev. 7, 48–55.
Tang, L., Ma, X.Y., Wang, Y., Zhang, S., Zheng, K., Wang, X.C., Lin, Y., 2020. Removal of trace organic pollutants (pharmaceuticals and pesticides) and reduction of biological effects from secondary effluent by typical granular activated carbon. Sci. Total Environ. 749, 141611.
Taylor, A.C., Fones, G.R., Mills, G.A., 2020. Trends in the use of passive sampling for monitoring polar pesticides in water. Trends Environ. Anal. Chem. 27, e00096.

Tchikuala, E., Mourão, P., Nabais, J., 2017. Valorisation of natural fibres from African baobab wastes by the production of activated carbons for adsorption of diuron. Procedia Eng 200, 399–407.
Teng, H., Lin, H.C., 1998. Activated carbon production from low ash subbituminous coal with $CO_2$ activation. Aiche J 44, 1170–1177.
Thakur, V., Sharma, E., Guleria, A., Sangar, S., Singh, K., 2020. Modification and management of lignocellulosic waste as an ecofriendly biosorbent for the application of heavy metal ions sorption. Mater. Today: Proc 32, 608–619.
Thue, P.S., Adebayo, M.A., Lima, E.C., Sieliechi, J.M., Machado, F.M., Dotto, G.L., Vaghetti, J.C.P., Dias, S.L.P., 2016. Preparation, characterization and application of microwave-assisted activated carbons from wood chips for removal of phenol from aqueous solution. J. Mol. Liq. 223, 1067–1080.
Tian, B., Li, P.F., Li, D.W., Qiao, Y.Y., Xu, D.P., Tian, Y., 2018. Preparation of micro-porous monolithic activated carbon from anthracite coal using coal tar pitch as binder. J. Porous Mater. 25, 989–997.
Tian, Y., Wang, F., Djandja, J.O., Zhang, S.L., Xu, Y.P., Duan, P.G., 2020. Hydrothermal liquefaction of crop straws: effect of feedstock composition. Fuel 265, 116946.
Tran, H.N., Nguyen, H.C., Woo, S.H., Nguyen, T.V., Vigneswaran, S., Hosseini-Bandegharaei, A., Rinklebe, J., Kumar Sarmah, A., Ivanets, A., Dotto, G.L., Bui, T.T., Juang, R.S., Chao, H.P., 2019. Removal of various contaminants from water by renewable lignocellulose-derived biosorbents: a comprehensive and critical review. Crit. Rev. Environ. Sci. Technol. 49, 2155–2219.
Tran, H.N., Wang, Y.F., You, S.J., Chao, H.P., 2017. Insights into the mechanism of cationic dye adsorption on activated charcoal: the importance of $\pi$-$\pi$ interactions. Process. Saf. Environ. Prot. 107, 168–180.
Valdivia-Garcia, M., Weir, P., Frogbrook, Z., Graham, D.W., Werner, D., 2016. Climatic, geographic and operational determinants of trihalomethanes (THMs) in drinking water systems. Sci. Rep. 6, 1–12.
Varsihini, J.S., Das, D., Das, N., 2014. Optimization of parameters for cerium(III) biosorption onto biowaste materials of animal and plant origin using 5-level Box-Behnken design: equilibrium, kinetic, thermodynamic and regeneration studies. J. Rare Earths 32, 745–758.
Velten, S., Knappe, D.R.U., Traber, J., Kaiser, H.P., von Gunten, U., Boller, M., Meylan, S., 2011. Characterization of natural organic matter adsorption in granular activated carbon adsorbers. Water Res 45, 3951–3959.
Verdugo, E.M., Gifford, M., Glover, C., Cuthbertson, A.A., Trenholm, R.A., Kimura, S.Y., Liberatore, H.K., Richardson, S.D., Stanford, B.D., Summers, R.S., Dickenson, E.R.V., 2020. Controlling disinfection byproducts from treated wastewater using adsorption with granular activated carbon: impact of pre-ozonation and pre-chlorination. Water Res. X 9, 100068.
Villaescusa, I., Fiol, N., Poch, J., Bianchi, A., Bazzicalupi, C., 2011. Mechanism of paracetamol removal by vegetable wastes: the contribution of $\pi$-$\pi$ interactions, hydrogen bonding and hydrophobic effect. Desalination 270, 135–142.
Wan, S.Q., Zheng, N., Zhang, J., Wang, J., 2019. Role of neutral extractives and inherent active minerals in pyrolysis of agricultural crop residues and bio-oil formations. Biomass Bioenergy 122, 53–62.
Wang, H.B., Zhu, Y., Hu, C., 2017. Impacts of bacteria and corrosion on removal of natural organic matter and disinfection byproducts in different drinking water distribution systems. Int. Biodeterior. Biodegrad. 117, 52–59.
Wang, J.W., Wu, B., Chew, J.W., 2020a. Membrane fouling mitigation by fluidized granular activated carbon: effect of fiber looseness and impact on irreversible fouling. Sep. Purif. Technol. 242, 116764.
Wang, T., Meng, D.X., Zhu, J.X., Chen, X.L., 2020b. Effects of pelletizing conditions on the structure of rice straw-pellet pyrolysis char. Fuel 264, 116909.
Wang, Y.M., Peng, C.S., Padilla-Ortega, E., Robledo-Cabrera, A., López-Valdivieso, A., 2020c. Cr(VI) adsorption on activated carbon: mechanisms, modeling and limitations in water treatment. J. Environ. Chem. Eng. 8, 104031.
Wang, Z.F., Lin, T., Chen, W., 2020d. Occurrence and removal of microplastics in an advanced drinking water treatment plant (ADWTP). Sci. Total. Environ. 700, 134520.
Wang, Z.H., Sedighi, M., Lea-Langton, A., 2020e. Filtration of microplastic spheres by biochar: removal efficiency and immobilisation mechanisms. Water Res 184, 116165.
Wei, X.C., Xue, X.F., Wu, L., Yu, H.Z., Liang, J., Sun, Y.F., 2020. High-grade bio-oil produced from coconut shell: a comparative study of microwave reactor and core-shell catalyst. Energy 212, 118692.
Wright, S.L., Kelly, F.J., 2017. Plastic and human health: a micro issue? Environ. Sci. Technol. 51, 6634–6647.
Wu, S.Y., Zhang, S.Y., Wang, C.W., Mu, C., Huang, X.H., 2018. High-strength charcoal briquette preparation from hydrothermal pretreated biomass wastes. Fuel Process. Technol. 171, 293–300.
Xie, N., Wang, H.M., You, C.F., 2021. Role of oxygen functional groups in $Pb^{2+}$ adsorption from aqueous solution on carbonaceous surface: a density functional theory study. J. Hazard. Mater. 405, 124221.
Yagmur, E., Gokce, Y., Tekin, S., Semerci, N.I., Aktas, Z., 2020. Characteristics and comparison of activated carbons prepared from oleaster (*Elaeagnus angustifolia* L.) fruit using KOH and $ZnCl_2$. Fuel 267, 117232.
Yahya, M.A., Al-Qodah, Z., Ngah, C.W.Z., 2015. Agricultural bio-waste materials as potential sustainable precursors used for activated carbon production: a review. Renew. Sustain. Energy Rev. 46, 218–235.
Yang, J., Qiu, K.Q., 2011. Experimental design to optimize the preparation of activated carbons from herb residues by vacuum and traditional $ZnCl_2$ chemical activation. Ind. Eng. Chem. Res. 50, 4057–4064.
Yang, K.B., Peng, J.H., Xia, H.Y., Zhang, L.B., Srinivasakannan, C., Guo, S.H., 2010. Textural characteristics of activated carbon by single step $CO_2$ activation from coconut shells. J. Taiwan Inst. Chem. Eng. 41, 367–372.
Yang, Y., Ok, Y.S., Kim, K.H., Kwon, E.E., Tsang, Y.F., 2017. Occurrences and removal of pharmaceuticals and personal care products (PPCPs) in drinking water and water/sewage treatment plants: a review. Sci. Total Environ. (596/597) 303–320.
Yang, Y., Zhu, J.J., Yang, L., Zhu, Y.Z., 2019. Co-gasification characteristics of scrap tyre with pine sawdust using thermogravimetric and a whole-tyre gasifier reactor. Energy Procedia 158, 37–42.
Yao, X., Xie, Q., Yang, C., Zhang, B., Wan, C.R., Cui, S.S., 2016. Additivity of pore structural parameters of granular activated carbons derived from different coals and their blends. Int. J. Min. Sci. Technol. 26, 661–667.
Yossa, L.M.N., Ouiminga, S.K., Sidibe, S.S., Ouedraogo, I.W.K., 2020. Synthesis of a cleaner potassium hydroxide-activated carbon from baobab seeds hulls and investigation of adsorption mechanisms for diuron: chemical activation as alternative route for preparation of activated carbon from baobab seeds hulls and adsorption of diuron. Sci. Afr. 9, e00476.
Yu, F.B., Zhu, X.D., Jin, W.J., Fan, J.J., Clark, J.H., Zhang, S.C., 2020. Optimized synthesis of granular fuel and granular activated carbon from sawdust hydrochar without binder. J. Clean. Prod. 276, 122711.
Yuan, T.Q., Sun, R.C., 2010. Modification of Straw For Activated Carbon Preparation and Application For the Removal of Dyes from Aqueous solutions. Cereal Straw As a Resource for Sustainable Biomaterials and Biofuels. Elsevier, Amsterdam, pp. 239–252.
Zaini, M.A.A., Zhi, L.L., Hui, T.S., Amano, Y., Machida, M., 2021. Effects of physical activation on pore textures and heavy metals removal of fiber-based activated carbons. Mater. Today: Proc. 39, 917–921.
Zhang, Z., Wang, T., Ke, L., Zhao, X.Q., Ma, C.Y., 2016. Powder-activated semicokes prepared from coal fast pyrolysis: influence of oxygen and steam atmosphere on pore structure. Energy Fuels 30, 896–903.
Zhang, Z.Q., Chen, Y.G., 2020. Effects of microplastics on wastewater and sewage sludge treatment and their removal: a review. Chem. Eng. J. 382, 122955.
Ziemba, C., Larivé, O., Reynaert, E., Huisman, T., Morgenroth, E., 2020. Linking transformations of organic carbon to post-treatment performance in a biological water recycling system. Sci. Total. Environ. 721, 137489.